Video and Laser Microscopy Investigation of Adhesive Joint Fracture in Fiber Reinforced Composite Materials

by

David H. Walworth

B.A., Liberal Arts
St. John's College, 1984

Submitted to the Department of Ocean Engineering in partial fulfillment of the requirements for the degree of

Master of Science in Naval Architecture and Marine Engineering

at the

MASSACHUSETTS INSTITUTE OF TECHNOLOGY

June 1996

Author .....
Department of Ocean Engineering
May 10,1995

Certified by .....
Koichi Masubuchi
Kawasaki Professor of Ocean Engineering
Thesis Supervisor

Accepted by .....
Professor A. Douglas Carmichael
Chairman, Departmental Graduate Committee
Department of Ocean Engineering

Video and Laser Microscopy Investigation of Adhesive Joint Fracture in Fiber Reinforced Composite Materials

by

David Walworth

Submitted to the Department of Ocean Engineering on May 10, 1996, in partial fulfillment of the requirements for the degree of Master of Science in Naval Architecture and Marine Engineering

Abstract

Adhesive bonding of fiber-reinforced composites is a common way of joining these materials. There are many advantages to this method, such as water- and air-tightness and the elimination of the stress concentrations which result from mechanical fastening methods. Adhesives transfer loads most effectively in shear, as opposed to tension. Consequently, any adhesive joints in composite materials will require an overlap of some type. Most joints used in marine applications, due to the ease of fabrication, are either lap joints, where the actual pieces overlap, or butt joints with doublers, where the structure's pieces are in line but doubler pieces overlap the joint line. This overlap in the joint immediately creates a discontinuity in the load path. A result of this overlap is a couple, which creates a bending moment, generating peel stresses at the ends of the joint. These peel stresses can be reduced by careful selection of the joint design, but they cannot be eliminated, except perhaps with the scarf joint. This type is not commonly used in marine applications as it requires extra machining time and therefore extra cost.

This study used two types of tools in order to gain a clearer understanding of adhesive joint fracture. These are video microscopy (VM) and a confocal scanning laser microscope (CSLM). The video microscope is a light microscope that will record an image directly onto a conventional VHS tape, creating a real time record. With this tool, the initiation and propagation of cracking can be recorded up to the point of final failure, which occurs more rapidly than the camera is capable of recording. This machine is highly portable and has interchangeable lenses for greater versatility. The CSLM is capable of actually measuring a surface profile. The ability to measure plastic deformation in the failed adhesive by examining the mismatch in the surface profiles of adjacent faces was explored.

Standardized carbon fiber reinforced plastic (CFRP) samples were joined by one of three different adhesives. The first, Gougeon 105, was chosen to represent a common boatbuilding epoxy. It was the most brittle of the adhesives. A second epoxy, Hysol EA 9430, was chosen to represent a more high tech adhesive, such as might be used in aircraft or custom yacht construction. The third, methacrylate ester, Plexus MA 550, is an adhesive that is becoming more common in marine applications. It is very ductile.

The continuous record afforded by the video microscope reveals the initiation of failure. There are three ways in which failure occurred for the samples: adhesive failure, cohesive failure, and interlaminar failure of the adherend. The existence of peel stresses and stress

concentrations at the ends of the joint predicted by other methods was observed.

The brittle Gougeon epoxy failed in adhesion, which was too rapid for the video microscope to record. The other adhesives exhibited some yielding behavior, through either interlaminar cracking, in the case of the Hysol epoxy, or distortion and then failure of the adhesive, as was the case with the Plexus adhesive.

The video microscope proved to be an useful tool to study the initiation of cracking in adhesive joints. The limiting factor is that there needs to be some type of yielding behavior, as opposed to rapid, brittle fracture. The laser microscope results were inconclusive. There was no correlation between the surface profiles of opposite faces.

Thesis Supervisor: Koichi Masubuchi
Title: Kawasaki Professor of Ocean Engineering

Acknowledgements

I would like to take this opportunity to thank Professor Koichi Masubuchi for his support throughout this project. It was gratifying to see the interest of a welding expert in an adhesive bonding project. Mr. Al Supple in the Technology Lab for Advanced Composites was very helpful and knowledgeable during the actual testing of the samples. To the numerous classmates who have helped me throughout my time here, I thank you.

My family has been a great encouragement. They have from the beginning encouraged continuing education and the learning of new things for all of their children. Eric Goetz and the rest of the crew at Goetz Custom Sailboats were helpful in the preparation of samples and the use of the shop to make samples. I would also like to thank an oft neglected group, the admissions committee. Thank you for the offer of admission, the time here has been both intense and rapid.

To my lovely wife, Dr. Michelle Peterson, for her encouragement and proofreading I owe incredible thanks. Not many women would have agreed to get married one month before the thesis due date.

Table of Contents

List of Figures

List of Tables

Chapter 1

Introduction

Adhesive bonding of fiber-reinforced composites is a common way of joining these materials. There are many advantages to this method, such as water- and air-tightness and the elimination of stress concentrations which result from mechanical fastening methods. Fiber-reinforced plastic (FRP)composites consist of a high-strength fiber in a plastic matrix, usually a polyester, vinylester, or epoxy resin. Stresses are transferred between fibers in a shear fashion by the matrix. A result of this is that a joint in a FRP material will always require an overlap of some sort, as it is with this overlap that the matrix transfers the stresses from one fiber to the next. Most joints used in marine applications, due to ease of fabrication, are either lap joints, where the actual pieces overlap, or butt joints with doublers, where the structure's pieces are in line but doubler pieces overlap the joint line. This overlap in the joint immediately creates a discontinuity in the load path. A result of this overlap is a bending moment, which is due to the couple created by the misalignment of the adherends. Normal, commonly called peel, stresses result at the ends of the joint. These peel stresses can be reduced by careful selection of the joint design, but they cannot be eliminated, except perhaps with a type called a scarf joint. This type is not commonly used in marine applications as it requires extra machining time and therefore extra cost.

To analyze the effects of these stresses, analytical models and finite element methods (FEM) have been utilized to study the fracture of adhesive joints. In addition, scanning electron microscopy (SEM) has been employed to study the propagation of cracks at discrete intervals and the condition of the fracture surface after failure. However, these methods can not make a real time, continuous record of an experiment. This study used two other types of tools in order to gain a clearer understanding of adhesive joint fracture.

These are video microscopy (VM) and a confocal scanning laser microscope (CSLM). The VM has the distinct advantage that it can make a continuous, real time record onto a conventional video cassette recorder (VCR) tape. This continuous record allows the review of an entire experiment at a later time, without necessarily having to predict at what time an individual image would have to be recorded. Later analysis and comparison of load and video data is also simplified as any point of the load data can be compared to the corresponding point of the video data. Another advantage of the video microscope is its portability. The unit is quite small and uses interchangeable lenses for greater versatility. The image is viewed on a separate monitor and also recorded, if desired, onto a conventional VCR tape. It was predicted that final fracture would occur too rapidly to record, but crack propagation up to the point of final failure could be recorded and studied. An examination was also performed into the use of the CSLM to measure the plastic deformation of the failed adhesives. The CSLM has the capability to measure a surface profile. The use of this capability to measure the plastic deformation of the failed adhesives by examining the mismatch in the surface profiles of adjacent failed surfaces of the adhesive was explored.

Chapter 2

Background

In the marine industry, the use of glass (GFRP) and carbon (CFRP) fiber-reinforced composites has come to dominate the small craft industry and found an increasing number of applications in larger craft. In the aerospace industry, FRP's have been used for many components, including ailerons and other control surfaces[1]. Joining the myriad pieces that go into the construction of a vessel or aircraft requires great care. This is due to the fact that at any joint there is some kind of discontinuity, whether it be a material or geometric discontinuity, and these can be the origin of failures. The traditional metal joining techniques of mechanical fasteners lead to problems of stress concentrations around the fasteners. Of course, if regular accessibility to underlying components is an issue, mechanical fasteners still have to be used. In a manner somewhat analogous to the transition from riveted to welded ships, the use of adhesive bonding to replace mechanical fasteners in composite structures has been on the increase. In addition, as these composite structures age, the necessity of repairs arises. The repair of damaged panels will almost always involve an adhesive joint, and the longevity of these repairs is an important economic issue[2]. Composites have even been tested to repair fatigue-damaged helicopter airframes, with the use of an adhesive joint between the composite material repair reinforcement and the aluminum of the airframe[3].

The analysis of the fracture characteristics of bonded joints has been the subject of numerous studies. Within the joint, it is the stresses at the ends that are of concern. Details at the end of the joint, such as spew fillets, rounding of sharp corners, tapering of adherends and plastic yielding of the adhesive can all significantly reduce the concentrations of shear and normal (peel) stresses at the ends of the joint[9]. There are

essentially three ways for a bonded joint to fail. One is for the bond between the adhesive and the laminate to fail, known as adhesive failure, the second is for the adhesive itself to fracture, which is known as cohesive failure, and the third is for the adherend itself to fail. As with other materials, there has been effort directed into nondestructive methods of testing joints[4,5]. Fracture mechanics theory has been used to examine and predict the behavior of the failure of bonded joints. Finite element analysis has also been used to analyze the stresses in joints, both basic joint designs and specific applications such as T-joints and top hat stiffener attachments.

2.1 Joint Types:

An important characteristic of adhesive joints is the presence of some type of overlap between the components being joined. This is in contrast to welded joints in metal, where overlaps are not required. The loads must be transmitted through an adhesive-adherend interface. The base material is called the adherend. The adhesive is the material used to join the adherends. There are two main types of adhesive joints: lap joints and doubler joints[6] (see Figure 2.1). A lap joint is a design where the actual material pieces overlap. The simplest of these is the single lap, oftentimes called a single lap shear (SLS)[7]. The double lap joint, in contrast, is symmetric, resulting in a joint that is more than twice as strong as the SLS, as it is a more symmetrically loaded configuration[8]. Two more complicated varieties are the scarf joint and the step joint[6], both of which require careful machining, but offer advantages of aerodynamic smoothness and lighter weight at all load levels[8]. An advantage to both the scarf and step joint is that the components are in the same plane, reducing the creation of peel stresses due to the out of plane centroid locations.

There are also several variations of doubler joints. The single doubler joint consists of a piece, the doubler, spanning the butt joint between two pieces. It is similar to a single lap

joint in terms of the asymmetry. A common use of this type of joint is for repair of aircraft skins and marine structures[8]. A double doubler joint is very similar to a double lap joint, with a doubler plate on either side of a butt joint joining two pieces of material (see Figure 1.1)[8]. With doubler joints, the main components are in the same plane, but the stresses are transmitted through the adhesive/doubler interface, through the doubler, then back through the adhesive into the main component (see figure 2.1).

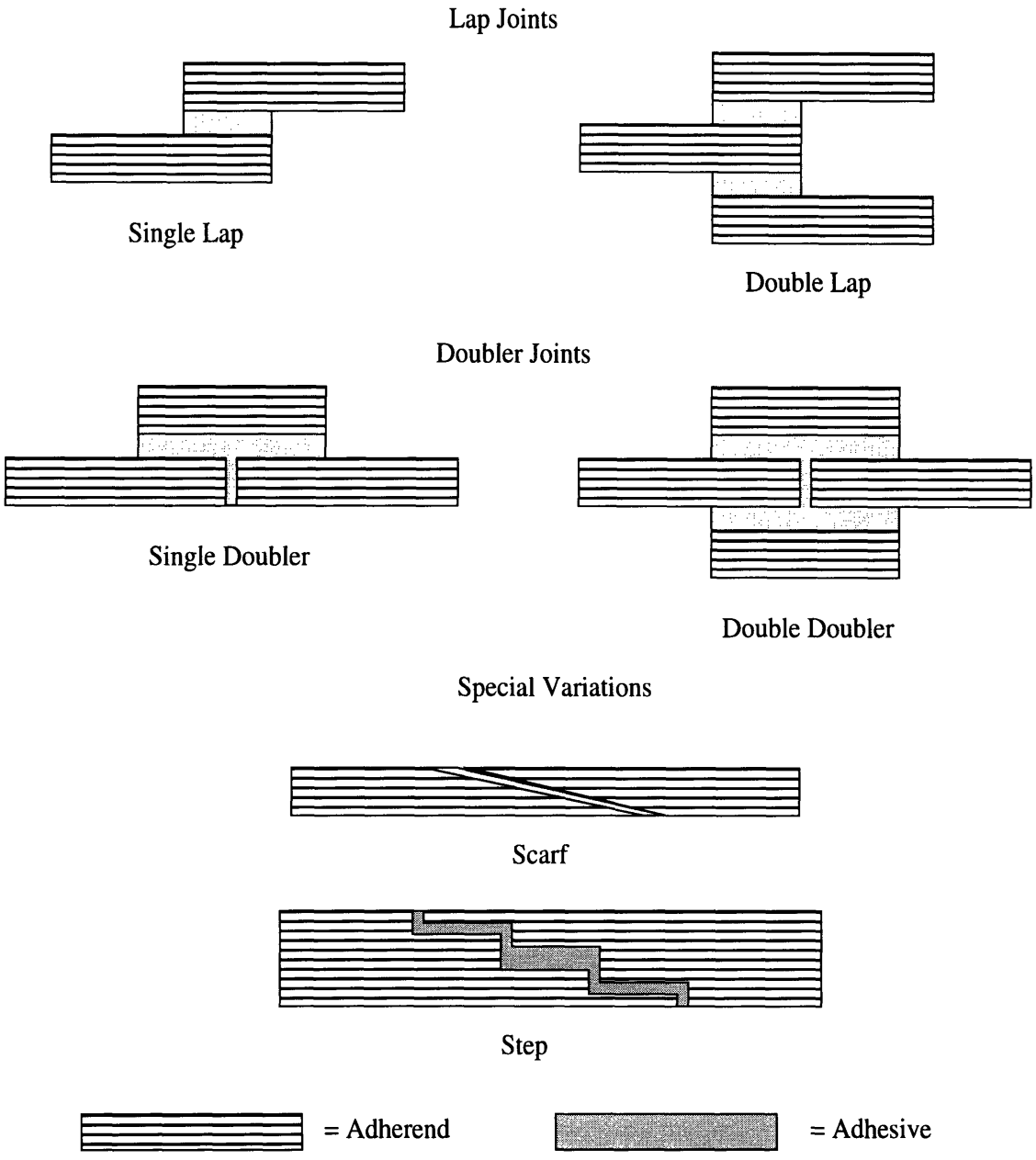

Figure 2.1: Joint Types, adhesive thickness not to scale

2.2 Analysis Techniques

The analysis of adhesive joints has been the subject of numerous studies. Two approaches that have been utilized are fracture mechanics and finite element method(FEM). Within the joint, it is the stresses at the ends that are of concern. Details at the end of the joint,

such as spew fillets, rounding of sharp corners, tapering of adherends and plastic yielding of the adhesive can all significantly reduce the concentrations of shear and normal (peel) stresses at the ends of the joint[9].

Peel stresses will occur in any lap or doubler joint This is true even for specimens loaded in tension. This is due to the difference in location of the centroids of the doublers and components. As a result, Mode I, opening, of a crack will always be a factor. Using a critical energy release rate method, the effects of the crack growth mechanism have been studied[10]. The critical energy release rate, Jc, was found to depend upon the mode ratio, the relative amounts of energy released in opening (Mode I) and sliding (Mode II) of the crack faces as the crack propagates (see figure 2.2) The dependence of Jc upon the mode ratio was determined experimentally, using a specially designed jig capable of giving pure Mode I to pure Mode II stresses for the adhesive systems under study. This gave a "fracture envelope" of the critical energy release rate versus the mode ratio. For any adhesive system, empirical data must first be obtained to create this fracture envelope. As

this fracture envelope is empirically determined, extrapolating the results of one adhesive system to another is not recommended.

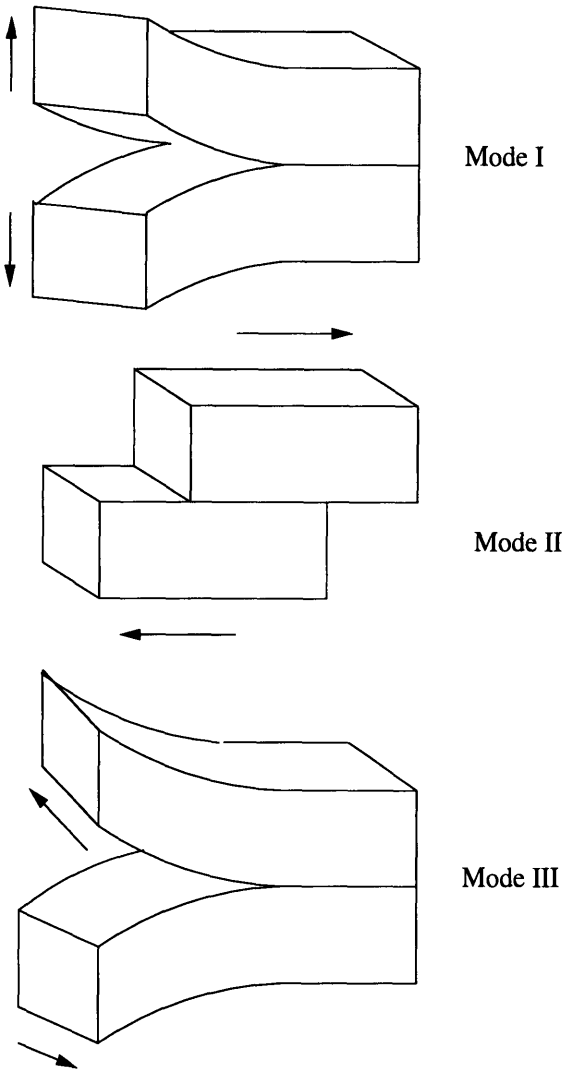

Figure 2.2: Modes of Failure

2.2.1 Fracture Envelope Technique

The fracture envelope technique was employed in studying both brittle and toughened epoxy adhesives. Once this fracture envelope was determined for the particular system, predictions of failure loads were made, and specimens were tested. It was found that the predicted versus experimentally determined failure loads differed by less than 10% for both brittle and toughened adhesives[10]. Given the fact that the fracture envelope was determined experimentally, it is not surprising that the values would be in close

agreement. Fracture propagated through the development of a "damage zone", rather than a sharp crack, with both types of adhesives. In the case of the more brittle adhesive, the load rate was found to have little effect. Tensile tests, using a cracked lap shear (CLS) specimen, exhibited a period of slow, stable "subcritical" crack growth of about 5 mm, after which the maximum load was reached and the joint fractured violently. The ductile adhesive exhibited a load rate dependence; Jc increased with an increasing load rate. The damage zone was also much larger. In tensile tests of a SLS joint, slow stable crack growth was observed over a distance of 7 mm, and then an increasing rate of crack growth was noted as the specimen slowly pulled apart. This is in contrast to the sudden, unstable crack propagation of the more brittle adhesive.

The effect of the thickness of the adhesive layer also requires consideration. Using the critical energy release rate technique, which is calculated from global joint properties, the thickness has relatively little effect[10]. This is due to the fact that the adhesive is usually only a fraction of the adherend thickness, thus having only a minor effect on the overall stiffness of the joint. However, experimental evidence indicates that there is an optimal range for adhesive thickness. In studies of shear fracture of adhesive joints, initially using adherends of either steel or aluminum, the critical energy release rate G reached a plateau maximum value at approximately 0.2 mm, regardless of adhesive type. The brittle samples also exhibited a decline in the critical energy release rate when the adhesive thickness increased beyond 0.7 mm. As the adhesive thickness decreased to 0, the critical energy release rates in all three modes, Mode I, Mode II, and Mode III (twisting shear), converged[11].

This dependence upon thickness has ramifications for composite joint design. As the Mode I energy release rates are much lower than Mode II or Mode III, optimizing the adhesive thickness for Mode I is critical. Fortunately, the peak energy release rate values

for all modes is achieved at the same value; ~0.2 mm for both the ductile and brittle adhesive. With the brittle adhesive, the critical energy release rate for Mode I did not appear to depend upon thickness, therefore using the optimal value for Modes II and III would be a logical design criteria. With the ductile adhesive, the mode I critical energy release rate actually exhibited a small peak around 0.2 mm, coinciding with the plateau value for Modes II and III. A suggestion was made that these findings could be used to help optimize the interlaminar toughness of composites. For shear loading, a simple technique suggested for interlaminar toughening would be to simply allow for a rich interlaminar resin layer (~0.1 mm)[11]. How this could be controlled during the lamination process was not addressed. A conclusion drawn from the results of this shear fracture study is that bond thickness be chosen to optimize the mode I critical energy, GIc, and the plateau value for the critical energy release rate, denoted Gsc [11]. The next step would be to minimize Mode I and maximize Mode II stresses by the design of the geometry of the joint.

2.3 Finite Element Analysis

Finite element analyses have been conducted of adhesive bonded joints to verify the fracture mechanics approach. The most common types of joints studied were the single lap, double lap, cracked lap shear (single lap joint with a starter crack), and double strap butt joints. Both tensile and bending tests were conducted, with the main focus on tensile tests. An analysis using a non-uniform mesh produced the best results, a fine mesh being required in the region of the crack tip and at the ends of the adhesive[12,13,14].A comparison of the results of an ASTM Round Robin study of two cracked lap shear joints, one with equal thickness (h1 = h2) adherends, CLS-A, and one with unequal thickness (h1 = 2h2)adherends, CLS-B, with the results of the energy release rate approach revealed that two non-linear finite element approaches yielded results very similar to the fracture

release rate approach used by G. Fernlund et al.[7]. The Round Robin study concluded that a geometrically non-linear analysis was required for these types of joints.

It was important to consider the boundary conditions. Reddy and Roy studied three cases, defined as Case 1, pinned-pinned ends, Case 2, pinned-free ends, and Case 3, clamped-clamped ends. Their results revealed that, in a joint of aluminum adherends with an epoxy (araldite) adhesive, for a Case 2 specimen, the stress distribution was considerably greater at the edges of the adhesive, as compared to the Case 1, or Case 3, which had similar stress distributions[11]. The adherends and adhesives were both assumed to be linearly elastic and isotropic.

Finite element analysis has also uncovered some interesting phenomena for double strap joints. Even in a symmetric joint such as a double strap joint, peel stresses are created due to induced bending moments in the strap adherends[7,13]. In the case of a double strap butt joint, the peel stresses were found to be very high at the doubler/adhesive interface, suggesting that this is where fracture would tend to initiate[13]. Even in a tensile-loaded joint, the doubler ends tend to bend upward, normal to the load direction. This suggests that it will be difficult to eliminate Mode I failure by joint design, although the likelihood of failure may be able to be reduced.

Studies of adhesive joint fracture using the fracture mechanics approach have been supported by the use of finite element analysis. A comparison of the results of an ASTM Round Robin study of two cracked lap shear joints, one with equal thickness ($h_1 = h_2$) adherends, CLS-A and one with unequal thickness ($h_1 = 2h_2$)adherends CLS-B, with the results of the energy release rate approach revealed that two non-linear finite element approaches yielded results very similar to the fracture release rate approach used by G. Fernlund et al.[7]. A conclusion of the Round Robin was that a geometrically non-linear analysis was required for these types of joints.

The effect of end conditions such as the adhesive spew fillet is unclear. Some investigators have concluded that the presence of the adhesive spew fillet has little effect on the fracture load, at least for double strap and single lap joint specimens. Fernlund et al.[7] feel that the reason for this is that steady-state conditions, which were used in defining the fracture envelope for an adhesive system, are not reached until approximately 5-10 mm of crack extension. However, Roberts reports that shear and normal stress concentrations at the ends of adhesive joints may be reduced significantly by details such as the rounding of sharp corners and the presence of spew fillets[9]. A possible explanation for these seemingly contradictory conclusions would be that the fracture envelope approach used by Fernlund et al. is determined after crack initiation, at which point the end condition details should have little effect. Given that most studies conclude that the stresses are concentrated at the ends of the adherend adhesive interface, one would suspect that the details of the end conditions would be important to the fracture load.

2.4 Adhesive-Adherend Interface

While the bulk of the studies have focused upon the fracture of the adhesive itself, some have also examined the composition of the adhesive-adherend interface. Many of the analyses of joint fracture have been performed using isotropic materials, such as aluminum or steel. Composites, however, are anisotropic materials. The tensile strength of fiber reinforced composites is much greater in the direction of the fibers. The orientation of the fibers at the interface has been found to play an important role in the strength of a joint[14]. Pradhan and colleagues conducted a study into the fracture of a double lap joint in CFRP. The analysis was conducted using the finite element method with paired nodes along the crack interface to compute the strain energy release rate[14]. For the purposes of analysis, only half of the joint was considered because of the symmetry of this type of joint. The geometric parameters were total length (Lt = 80 mm), overlap length (Lo = 40

mm), adherend thickness (tr = 10 mm), adhesive thickness (ts = 2 mm) and critical strain energy release rate (Gc = 0.06 kJ/m2). These parameters were all held constant for this study. The problem was treated as a plane strain problem. Material properties of the adherend were (El = 137 GPa, Et = 7 GPa, Glt = 4.5 GPa, lt = 0.3) and the adhesive was (Es = 3.5 GPa, = 0.41). Three non-dimensional parameters were also defined; E = Er/Es, L = Lt/Lo, and t= tr/ts. Er and Es designate the elastic moduli of the adherend and adhesive, respectively. For this study, Lt, tr, and Er were held constant in all of the tests. This approach allowed optimal values of E, L, and t to be determined. A general conclusion was that a 0^{o} layer at the adhesive interface resulted in a stronger joint. Other characteristics found to be desirable were a low moduli ratio E, low overlap ratio, L, and high thickness ratio, t[14]. In the application of these conclusions, one has control over E in the materials selection process and t and fiber orientation in the design process. However, in a structure of any size, the value of L will rapidly become large. A relationship of Lo to adherend thickness would be more useful, although the implications are clear; the longer the overlap the better.

2.5 Studies of Specific Joint Designs:

There have been investigations into specific applications of typical joint designs used in the marine industry. These are T-joints, such as a bulkhead to hull joint[15,16,17], and "top hat" to hull joints, a design typically used for stiffeners[18]. For the top hat study, the investigators were interested in the practicality of using pre-made sections and joining them to the hull, as opposed to the current practice of building a stiffener in place over a foam core, as the use of prefabricated sections has the potential for considerable labor savings. The study of T-joints and top-hat joints covers the vast majority of the joints in a typical FRP boat or ship. All of these investigations were undertaken with the goal of coming up with an analysis approach to be used in the design phase of a vessel.

For both T-joints and top-hat stiffeners there are two main variables to the joint design. These are the radius of the fillet and the thickness of the overlaminates (see figure 2.3). The fillet is thickened resin in the corner of the joint, it has the purpose of both joining the components and providing a smooth transition for the fibers of the overlaminates joining the components. The overlaminates are fiber reinforcement across the joint. In some cases, just a fillet is used. These tend to fail rather catastrophically[18].

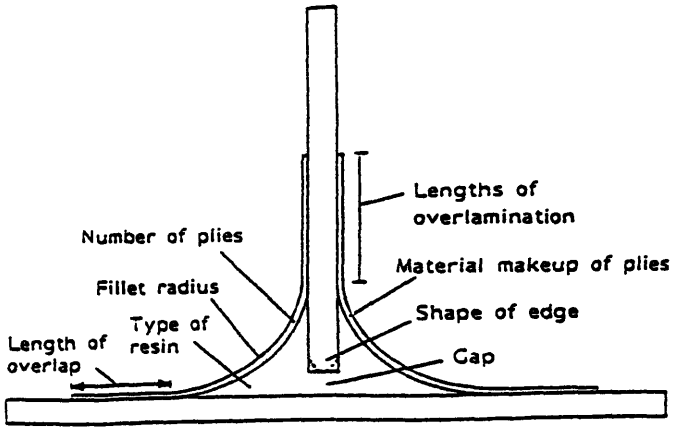

Figure 2.3: T-joint Design Variables[17]

All of these investigations used FEM as an approach to analyze the stresses in the joints. A common problem stated by all of the investigators is the lack of a data base with which to compare the results. As a consequence, the FEM results were compared to experimental data obtained by the investigators. Another variable is that in two of the T-joint investigations used sandwich panels as the panels being joined. Thus a third material, the core, was introduced. Cored sandwich construction is a common technique for high speed craft such as planing powerboats and racing sailboats. The third T-joint

investigation was oriented towards large ship construction utilizing solid glass laminates, such as would be used in a minesweeper. The top-hat design analysis was also undertaken in the context of large vessel design, where cost of construction might be more of a consideration than in a high speed racing craft, where weight efficiency is a primary consideration.

Three different loading situations were studied for the T-joint tests. These were lateral loading of the web of the T, tensile loading of the web, and compressive loading of the web of the T, such as would occur in slamming. Five different types of attachment were studied for the compressive loading. These consisted of a foam pad with beveled edges, upon which the web piece sat, triangular foam inserts, in lieu of fillets, and three different fillet radii; 10 mm, 25 mm, and 40 mm. For compressive loading, it was found that the small 10 mm radius gave the best results in terms of experimental versus predicted values (8% greater than predicted) and from both the weight and production efficiency standpoints. The foam pad gave the next best results, but the production efficiency is worse as the foam pad pieces are particularly difficult to cut[16]. The authors stressed that these results were for joints loaded in compression only, and that the results could very well be reversed in another type of loading, such as a side load applied to the bulkhead. In all of the cases, the failure initiated with local buckling of the panel face at the edge of the overlaminate. The large fillet not only gave relatively poor performance but was expensive to manufacture due to the large quantity of epoxy resin required. The tensile loaded web was also an analysis using cored panels. The investigators observed two major failure modes in this situation:

I) Failure in the laminates, the core of panel A (the web or bulkhead), the glue, and the attachment lap.

II) Shear fracture of the core in panel B (the hull).[15]

For the purposes of the study, linear elastic behavior was assumed, with no defects. Four areas of stress concentration were identified; one each at the interface of the fillet, overlaminate, and panel face, one at the end of the web panel skin fillet interface, and one at the end of the web panel skin/core interface. FEM was used to analyze the joint, with a fairly fine mesh, and assuming plane strain. The most critical stress, relative to the ultimate material strength, is in shear for the core of the web panel A where the skin, core, and adhesive meet. This tensile analysis was not very satisfactory. No data in terms of experimental loads at failure or modes of failure were provided to quantify the predicted values[15]. Neither analysis gave overlaminate thickness recommendation, although the compressive test experiment gave a rule of thumb that the optimum filler radius should be chosen to be approximately the thickness of the sandwich panel. Which panel to use if there is a great difference in thickness was not indicated, although their results would imply to use the thinner panel's thickness. ABS (American Bureau of Shipping) is not much help either, the only recommendations are for bulkheads, which "are in general to be glassed-in on both sides and the thickness, strength, and overlap of the tapes or angles are to provide strength and stiffness equivalent to the shell or deck laminates to which they are being attached.'[19]

The tests carried out upon the solid laminate configuration employed a bending load upon the bulkhead. The specimens consisted of thick overlaminates, thin overlaminates, and no overlaminate designs. The authors propose the thin overlaminate design as being a potential replacement for the thick overlaminate configurations, two main variations of

which are currently in practice, at least in the U.K. where this study was performed (see figure 2.4).

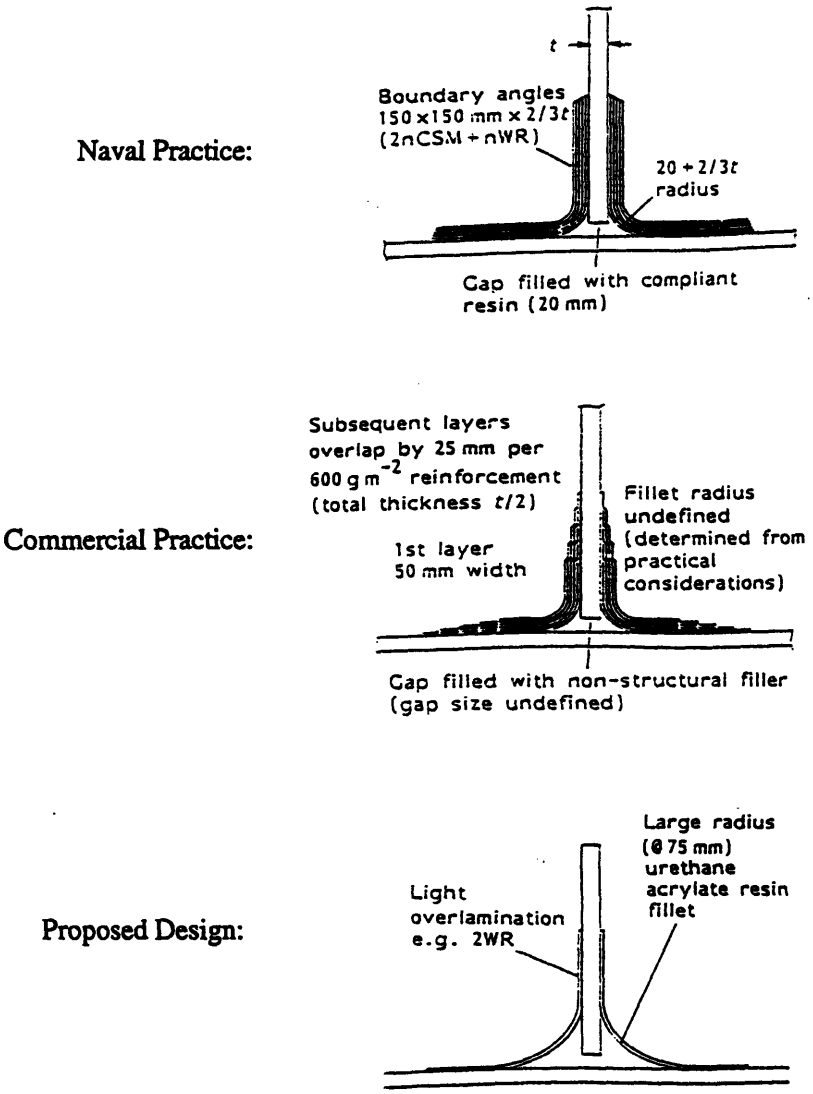

Figure 2.4: Current and Proposed T-Joint Designs[17]

The authors also suggest using a tougher resin for the fillet, as GRP (Glass fiber Reinforced Plastic) laminates, the focus of their tests, have a low modulus and are relatively flexible. The toughened urethane-acrylate resins they propose using have a

lower ultimate tensile strength than polyester resin but a much higher elongation to failure. This flexibility was felt to be important as "traditional GRP boundary angles are not flexible enough to alleviate peel loads," especially in a joint that might be subjected to through thickness tensile stress[17]. Two other parameters that were investigated for their relative importance were the thickness of the gap between the web and the flange piece and the configuration of the end of the web, whether cut square or beveled.

Seven different configurations were tested to provide information as to the effects of the different parameters. The samples were tested by being subjected to a displacement-controlled pull-off at 45° to the base plate. This created one tension, one compression side. Two were typical naval practice, one with an overlaminate using polyester resin (sample A) and one with the urethane acrylate resin (sample B), both overlaminates being thick (2/3 the thickness of the flange). Three samples consisted of 75 mm fillets of just urethane-acrylate resin, one with a gap of 15 mm and square cut edges (sample C), one as C only with a 25 mm gap (sample D), and one as C but with a 6 mm bevel edge to the T piece (sample E). The remaining two samples were as C with a light overlaminate of two layers of E-glass woven roving with a polyester/urethane-acrylate resin mix (sample F) and as C but with the fillet radius increased to 100 mm (sample G). It was found that the thick overlaminates failed initially within the plies of the overlaminate, at which point the load carried by the joint dropped away to a very small amount. Increasing displacement resulted in the joint continuing to carry load with little reduction in stiffness to a level higher than initial failure until complete failure occurred when the remainder of the overlaminate plies delaminated. Sample B behaved in a very similar manner to A. Sample C failed catastrophically and rapidly, making it hard to observe the actual failure mechanism. D showed large cracks and variations in stiffness before failing catastrophically. E failed similar to C. F failed catastrophically by complete delamination

of the overlaminate and cracking of the fillet. The speed at which these events happened was too great to distinguish the order of initial failure. G also failed catastrophically. The conclusions were that increasing the gap allowed much greater deflections before failure, allowing the joint to absorb more energy, bevelling the end reduced joint stiffness but increased failure load by over 50%. Overlaminating increased stiffness by 50% and failure load by 100%. Increasing the radius of the fillet made little stiffness difference but increased failure load by 150%[17].

The investigators then used FEM to analyze the samples. The purpose was both to investigate the internal strain patterns of the samples and to provide a verification of the FEM procedure. It was found that the FEM analysis overpredicted the stiffness but was able to differentiate between the different flexibilities of samples C,D, and E, despite the quite small variations of the geometry. The large deflection analysis did not correspond to the experimental values. It was postulated that the material properties were incorrectly modeled and a reiteration with different material properties was done as a check. The results were in much closer agreement[17]. This suggests that the FEM analysis can work but that it is sensitive to the material properties, particularly the linearity of the material properties.

To study the stress regimes only the three major configurations were tested. These configurations were represented by samples B, C, and F.The analysis indicated that the configuration most efficient was sample F. The thin overlaminate configuration tended to distribute the load most evenly between the overlaminate and the fillet. Another conclusion reached was that similar deflection samples tended to have similar loads to failure. The authors introduced the concept of "joint efficiency." This basically means that the joint with the lowest stress levels for a given load and deflection is the most efficient. Sample F was the design that met this criterion[17].

In their conclusion, the authors make three main points. These are first that the joint is heavily dependent upon geometry and material makeup. The second point is that FEM analysis is not reliable at this point(1992) due to the incomplete nature of material data, as evidenced by the necessity of adjustments to the material data being performed. As a material property database is developed, this weakness should be reduced.The third point was their conclusion that the most efficient joint is contrary to current practice; a thin overlaminate of minimal thickness, just sufficient to withstand the membrane loads, as opposed to the thick overlaminates in current use[17].

The comparison of the top-hat stiffener construction techniques was primarily to see if the approach of using the prefabricated pieces was viable, as compared to the current practice. Currently, top-hat stiffeners are fabricated in a fairly labor intensive process. A foam former is first glued to the hull panel. Then the overlaminate is applied, sometimes with a layer or layers of unidirectional fibers along the "flange" (parallel to the hull surface) face. The authors investigated the use of prefabricated u-section stiffeners trimmed to fit the hull and bonded in with a fillet and overlaminate of 2-3 layers of woven roving. The two developments that make this procedure a possibility are the increasing availability of prefabricated sections and the development of a mechanized gun to form the fillets. The authors addressed two questions, the mechanisms of load transfer and the impact of variations of geometry upon the strength of the joint. The latter investigation was especially relevant to variables of the manufacturing process. Previous work has shown that the joint is strong during in-plane loading but is the weak link in out of plane loading[18]. Testing with the application of tensile forces has received the most attention as the primary problem during out of plane loading has been joint debonding, as opposed to web buckling. Two types of loading were considered; center clamp and two clamp loading. Center clamp loading applies a tensile load to the flange or "table" of the top hat

while restraining the plate in the center of the top-hat section. This has been more commonly used as it results in the lowest failure load. However, in service the vessel is unlikely to see this situation as the width of the unsupported plate is generally much larger than the top hat table. Center clamp loading also does not result in premature delaminations in the overlaminate. Two clamp loading clamps the plate with a clamp on either side of the stiffener. This simulates the situation of a tank during pressure testing or the situation when a shock bubble implodes, resulting in a negative exterior pressure. The premature delaminations resulting from these tests are in agreement with the delaminations seen in actual conditions[18].

The study primarily addressed the design variables affecting the strength of the joint. These are fillet radius, overlaminate thickness, gap between web and plate, and backfill angle of the fillet. Their conclusions showed that gap size and backfill angle had little effect on the performance of the joint. These are also the two variables most difficult to control, as they would be dependent upon the skill of the worker. It was also found that both fillet radius and overlaminate thickness could be optimized for a given application. Increasing fillet radius and decreasing overlaminate thickness reduces through thickness stresses in the overlaminate, reducing the problem of delamination in the overlaminate. This is similar to the conclusions reached by the same authors in their study of bonded T-joints[17, 18]. The important implication here is that as far as the state of the art goes, there is an indication that light overlaminates, which is completely at odds with the current practice, could be the optimal joint design for these applications. However, these are only two studies. Curiously enough, in the study of bonded T-joints for small craft, with cored panels, decreasing the fillet radius was found to be the more optimum approach, although it must be remembered that study was for compressive loading of the web[16].

2.6 Non-Destructive Testing Techniques:

As with any type of joint, it is desirable to be able to non-destructively test the integrity of a bonded joint. Certainly it is more desirable to detect weakened bondlines before failure, rather than detecting them with failure. An interesting development is the use of holographic interferometry[4]. This technique is to detect flaws, as opposed to testing for the ultimate strength of a joint design. What is particularly interesting is that the authors of the study approached the problem of detecting flaws from the stiffness standpoint. The technique involves taking a holographic image of the joint as it is subjected to loads at 1kn increments. Debonded areas were purposely introduced by the use of teflon disks and oil smears. The adherends in this study were aluminum, but this technique would probably work as successfully on composite adherends. The debonded areas show up as out of plane contours in the hologram. While the authors do not suggest this, it could be possible to use this technique to monitor the condition of structures in service. If a record is kept of the structure when built and then regular holograms were taken of the structure or at least key elements of the structure, the holograms could be compared to the when built images. A significant change in the hologram would serve as an indicator that degradation of the joint had progressed to a certain point.

The authors also used the hologram results to help model the way in which stresses are transferred in a bonded joint with flaws. The authors have observed that more shear stress is taken by the good side of the bondline, when only one face has an induced flaw. They even postulate that the good bondline could be the one to ultimately fail due to the higher induced load. As other authors have concluded, peel stresses are pretty much a fact of life for bonded joints. They have proposed, understandably, that peel displacement would be greater on the side of the joint with the bondline flaw. An equation has been derived to express the bondline peel stiffness, k_b;

$$\frac{1}{k_b} = \frac{1}{k_{int}} + \frac{1}{k_a} + \frac{1}{k_{int}} \tag{2.1}$$

where k_{int} represents the stiffness of the interface and k_a represents the stiffness of the adhesive. Bondline peel stiffness can then be expressed as:

$$k_b = \frac{k_a \cdot k_{int}}{2k_a + k_{int}} \tag{2.2}$$

Therefore as $k_{int} \to \infty, k_b \to k_a$ and if $k_{int} \to 0, k_b \to 0$, which situation represents a debond. If $k_{int} = k_a, k_b = k_a/3$, which is the epoxy rich layer of the composite adherend.

This approach appears to have potential as a good Non-Destructive Testing (NDT) method. While insight has been gained into the study of peel and shear stresses in bonded joints, expressed as a function of stiffness, it seems that the great strength of this technique could be in testing. The stiffness of the joint, both in-plane and out-of -plane, is reduced if the joint integrity has been degraded. This loss of stiffness can be detected at low non-destructive loads[4]. Even the location of the flaw, to some extent, can be determined with the holographic interferometry technique, as the images will be different on the degraded versus the intact side.

Currently, acoustic testing techniques do not seem to perform very well in the evaluation of bonded joints with composite adherends. This is primarily due to the fact that the adhesive is quite often similar to, if not the same as, the matrix of the adherend[5]. Acoustically, it is hard to distinguish the bondline from the inter-laminar matrix resin. Gross defects can be detected, such as major debonds, but any evaluation of the cohesive properties of the adhesive is hard to determine for the composite adherends situation. For an adhesive joint with metal adherends, the acoustic signatures are quite different for the adhesive and adherend, in that case evaluating the properties of the adhesive can be more

easily performed. In terms of NDT methods, the holographic interferometry method seems to show more promise, as it measures stiffness of the joint.

2.7 Repair:

As structures age, the necessity for repairs arises. This is as true for composites as it is for any other material. A repair in a composite part will by necessity involve a joint of some type, most likely bonded. When the structure is originally manufactured, the conditions are usually fairly controlled, particularly from the standpoint of moisture content. Once a part is damaged, the likelihood of moisture or oil contamination of the surface must be considered. When a part is manufactured or repaired using heat curing adhesives, the heat helps to remove contaminants through the combination of high pressures in the autoclave, low pressures within the vacuum bag, and the heat applied for curing, all of which contribute to the vaporization of contaminants such as water or oil[2].Repairs, however, are oftentimes carried out in non-ideal conditions, with cold cure (room temperature) adhesives. Autoclaves are expensive, and sometimes it is not practical to repair a part using an autoclave. For instance, if the wing panel of an aircraft is damaged and it is desired to repair it in place, the piece would not fit inside an autoclave, as that would require an aircraft sized autoclave. Sometimes, particularly in the aircraft industry, repairs are made with cold (room temperature) cure adhesives. These would be classified as temporary repairs, with the consequent added expense of redoing them at a later date. In an effort to ascertain just how temporary these repairs were, an investigation was undertaken into the longevity of repairs made under typical field conditions. The investigators had two main objectives; to ascertain the effects of absorbed moisture on initial adhesion and the long term durability of cold cure adhesive joints in relatively harsh environments (90% relative humidity, 40^{o}C)[2].

A question that arises in a repair is the effect of moisture in the underlying laminate. The surface can be dried, but moisture could still be present in the interior layers. This moisture could migrate to the repair joint and detract from the longevity. To investigate the effects of moisture and temperature on the properties of an adhesive, samples were aged at 90% relative humidity and 40° C for several months. The authors of the report investigated the performance of double lap joints of prepreg composite adherends with room temperature cure adhesives. They investigated the susceptibility of the joints to long term environmental effects, both heat and humidity and immersion in oil and also the effects of moisture contamination of the underlying surface. To examine the effects of moisture contamination upon the joint strength, specimens were dried for various intervals of time up to fourteen days at 80°C. It was found that drying time had little effect upon the joint strength, presumably as long as the surface at least was not wet at the time of bonding. The effects of immersion in oil upon the strength of an already bonded joint was also investigated. This is an important parameter as it is certainly possible that immersion in oil could happen in either a marine or aircraft structure. However, aging times of up to three months showed no significant change in joint failure load[2]. These results indicate that surface contamination by water before the repair is made and oil immersion of the completed joint have little effect upon the strength of the joint. This is promising for the satisfactory performance of field repairs.

The effects of long term exposure to moisture was also studied. Completed joints were exposed to aging conditions of 90% relative humidity and 40°C for up to twelve months. Both experimental results were obtained and finite element predictions were made. The results were in good accordance with each other, indicating that the material properties chosen for the finite element model were good. It was found that the total loss of strength due to aging in a hot wet environment would eventually cause a total loss of strength of

approximately 30% over the unaged values. Presumably this could be allowed for in the design of the repair. The conclusion reached by the investigators was that "the main mechanism of environmental attack is via water ingress and the plasticization of the adhesive and matrix of the fibre composite." This conclusion was reached by observing the modes of failure[2]. While the authors make no final recommendations as to the categorization of room temperature cure repairs in terms of permanent versus temporary, it seems as if it should be possible to categorize the repairs as permanent if the degradation due to aging is allowed for in the design. The fact that surface contamination seems to have little effect, as long as the surface is cleaned and dried, helps to support the view that these repairs can be classified as permanent. Moisture contamination of the damaged surface would be almost guaranteed if it was a marine structure. Experience has also shown that repairs in composite material structures can be long lived. For example, in January of 1991,an IOR 50 foot class racing yacht was damaged in a collision to such an extent that twenty feet of the forward section of the yacht had to be cut off and completely replaced. This involved a joint all the way around the circumference of the hull. This yacht is still sailing today and went on to win the Fastnet race and Admiral's Cup in 1991 with no problems[20].

An interesting use of composite joining has been in the repair of cracked helicopter fuselages. In a fatigue study conducted in the U.K., a helicopter fuselage was fatigue tested to failure. The resulting cracks were repaired with CFRP bonded directly to the surface. Subsequent testing showed fatigue lives of these repairs as being greater than the original life of the structure. Criteria for a successful repair were also developed as a result of these tests. Cracked flanges of the webs were generally repaired with unidirectional layups. Webs were generally repaired with +/-45^{o} laminates and any lightening holes were filled with foam core[3]. An advantage to these composite repairs is that they can be done

in place and there is no heat involved, which is important for a structure that is manufactured out of heat treated aluminum. Even if the aluminum is not a heat treated alloy, welding would still introduce distortion.

2.8 Design Rules:

Simplified procedures have been developed for the design of bonded joints. These rules can take into account static and dynamic loads and also adverse environmental effects[6]. Essentially there are three main parameters which are considered. These are; minimum length of overlap, l_{min}, maximum shear stress in the adhesive, σ_{as}^{max}, and the

maximum peel or normal stress in the adhesive, ρ_{an}^{max} . Equations for the various configurations of joint design have been developed, as can be seen in figure 2.5.

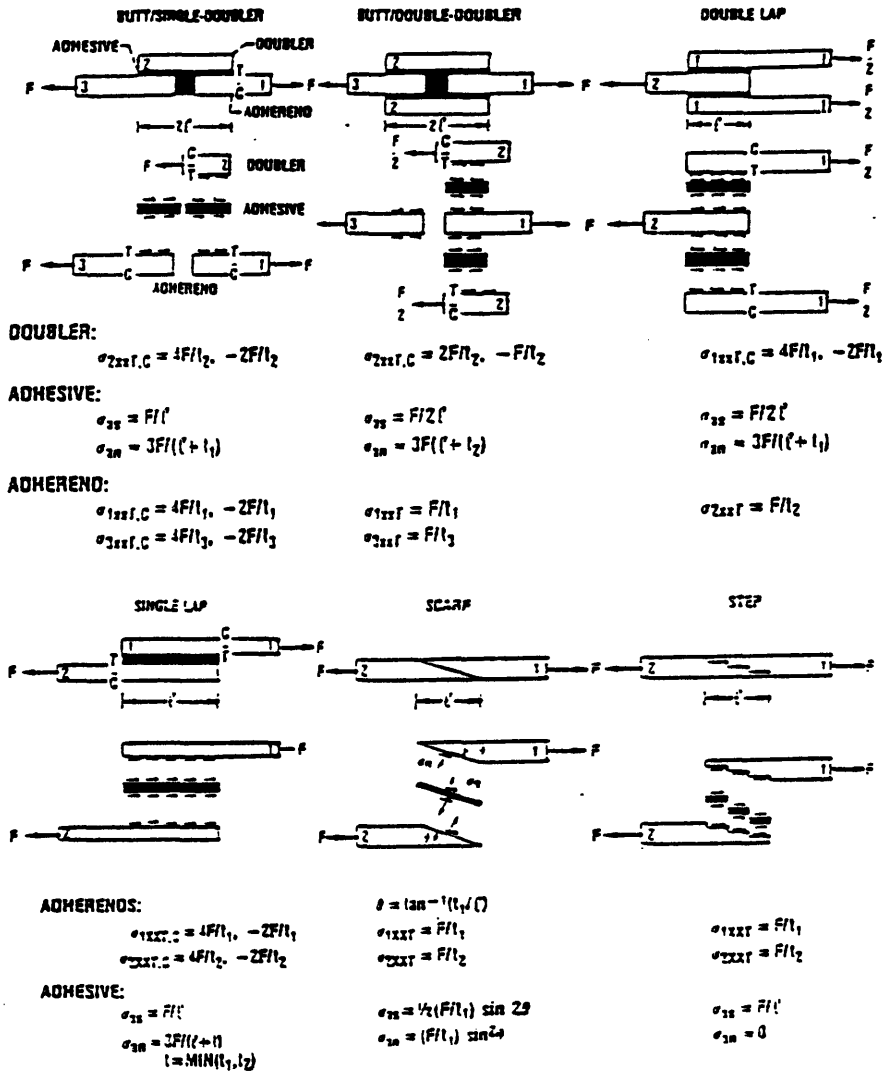

Figure 2.5: Equations of Stress for Various Joint Configurations[6]

Using these equations, a series of steps can be followed in order to determine the minimum overlap length required. Once a joint type has been decided upon and an adhesive-adherend combination selected, the only real variable left is the joint overlap. It

is this overlap length which is determined from this simplified procedure. The specific steps are as follows:

1) Establish the joint design requirements, the loads, laminates, adhesive, safety factors and any special design considerations.

2) Using composite mechanics the laminate dimensions and properties for the adherends are obtained.

3) Obtain the properties of the adhesive. In many cases, the adhesive is the same or very similar to the matrix of the adherend. The shear strength and peel strength are the properties of interest.

4) Degrade the adhesive properties for environmental and cyclic loads. For a simple dry, static loading test this step can be omitted, which simplifies the process in the early stages of design. However, these degraded properties of the adhesive will need to be used in the more detailed analysis. The following equation is used to determine the degraded values for the adhesive:

$$\frac{S_a}{S_{ao}} = \left(\frac{T_{gw} - T}{T_{gd} - T_o}\right)^{1/2} - 0.1 \log N \tag{2.3}$$

These variables are as follows; S_a is the expected adhesive strength being calculated for a particular loading environment, S_{ao} is the corresponding strength at reference conditions, generally room temperature dry, T_{gw} is the wet adhesive glass transition temperature, which is obtained by this equation:

$$T_{gw} = (0.005M^2 - 0.1M + 1.0)\, T_{gd} \tag{2.4}$$

M is the moisture content in the adhesive, in percent by weight. T_{gd} is the dry glass transition temperature, usually obtained by the adhesive supplier. T is the temperature of the joint in service, T_o is the reference temperature at which S_{ao} was determined. Usually

this temperature is room temperature. N is the number of cycles which the joint will endure at the design stress.

5) Design allowables must then be selected. These can be set by either the design criteria or chosen using two different techniques: (a) put a load factor on the force F, this factor is often 1.5 or 2.0, or (b), use a safety factor of one-half of the degraded strength of the adhesive, S_a, determined from step four. As F may already contain a load factor, the second alternative is recommended.

6) Now, the overlap length l of the joint must be determined, using this equation:

$$l = \frac{F}{S_{as}} \tag{2.5}$$

F is the load in the adherends per unit width and S_{as} is the design allowable shear stress in the adhesive.

7) The minimum length and maximum shear and normal stresses in the adhesive are checked using the shear lag equations in figure 2.6.

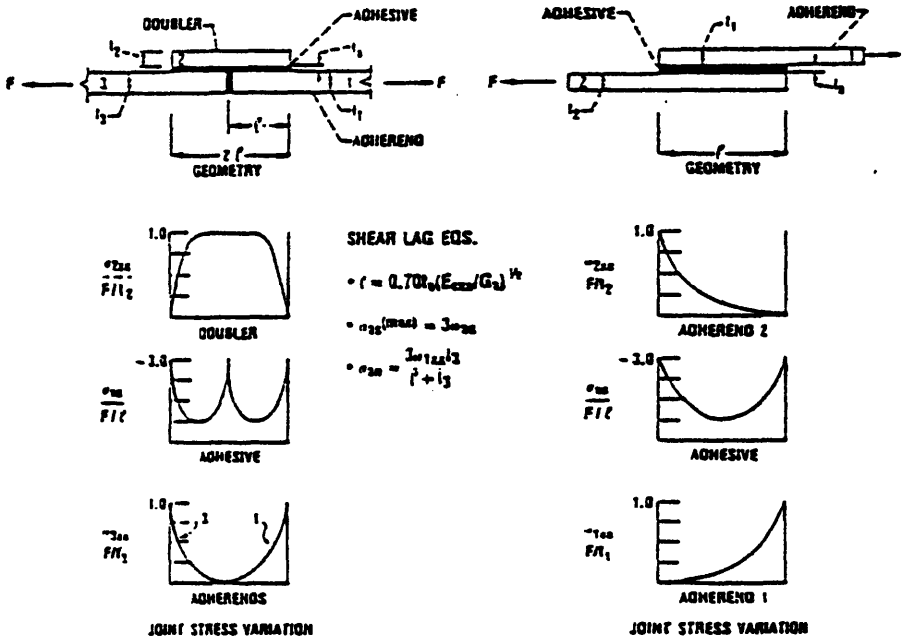

Figure 2.6: Shear lag equations for single doubler and single lap joints[6]

8)The bending stresses in the doublers and adherends are calculated using the respective equations for the type joint (see figure 2.5).

9) The margin of safety (MOS) is then determined for all of the calculated stresses. Usually this is performed at each step where stresses are calculated and compared to the allowable stresses using this equation:

$$MOS = \frac{AllowableStress}{CalculatedStress} - 1 \tag{2.6}$$

10) The joint efficiency (J.E.) is calculated with this equation:

$$JE = \frac{F}{S_{cxxT}} \times 100 \tag{2.7}$$

In this case F is the joint force transferred and S_{cxxT} is the adherend fracture load, determined in step two using composite mechanics.

11) Finally, the joint design is summarized[6].

Two examples are calculated, one with just a static no environmental effects load and then the same joint allowing for environmental loads and cyclical loads. The type of joint was a butt joint with a single doubler. It turned out in the example that the calculated overlap length was so small that it was increased arbitrarily from 0.12 inches to 1.0 inches. All other conditions were satisfied with substantial margins which indicates that this type of joint is not very efficient. An important observation is that the joint length predicted using shear lag is practically negligible, which indicates that the load transfer occurs in a very short distance[6]. Calculations of bending stresses were also within safety margins. These calculations of in plane loads were preliminary, a more detailed analysis would then be performed using laminate analysis to calculate the ply stress. For this type of joint the ply stress calculations indicated that the simple approach was conservative. The joint efficiency was quite poor, which is typical of all joints that induce bending in the doublers and adherends[6]. If the structure configuration allowed it, the use of a joint design that reduced the bending stresses would be preferred.

This same joint was then examined for suitability using degraded properties. As the design was not changed, the properties were just degraded. For this particular example, the required joint lengths were substantially increased, about 2.5 times. However, due to the decision to arbitrarily increase the overlap length, this joint design was still adequate. An important observation made here was that the bending stresses are not substantially affected if 0^o plies are placed next to the adhesive. This results from the fact that fiber

dominated properties are not sensitive to moisture or temperature degradation[6]. This recommendation to place 0^o plies next to the adhesive has been noted in other literature[14].

The steps followed are applicable to all of the composite joint designs. For preliminary design they appear to give good results, and would be helpful in deciding upon candidate designs for closer study. After the preliminary design(s) have been decided upon, then a more detailed finite element analysis would be carried out. If the joints are of a type that induce bending, care must be taken to select a model with enough joint length to simulate bending. Usually a unit width model with plane elements through the adherend and adhesive thickness is sufficient[6].

2.9 Current state of the art summary

The state of the art of adhesive bonded composite joints is in a rapidly evolving stage. This would be expected from a field such as composites that is still expanding. Tools such as finite element analysis have been found to be effective, with careful consideration paid to the properties of the materials[17]. Simplified guidelines for the design of composite bonded joints have been developed[6]. These simplified guidelines are useful as it allows a designer to design a structure with confidence without having to resort to first principles to be confident that the design is adequate. A basic observation made by many researchers is that peel stresses should be minimized, as the Mode I type of peel failure occurs at the lowest loads. However, these peel stresses cannot be entirely eliminated[7] and must be taken into account. In general, asymmetric joints are inefficient, and should be avoided if at all possible. There is less agreement upon the importance of details. Some researchers reports that end details have little bearing on the fracture load[10]. Others report that the details at the ends of the joint are significant[9]. However, since fracture will begin at the

ends of the joints, it would stand to reason that end details which would help to reduce peel stresses would have an effect upon the fracture load.

An indication of a maturing of the field is that there has been research into the design of specific joints. In particular the design of stiffener attachments and T-joints, both of which are incredibly important to the construction of a ship. What is interesting is that these studies indicated that the current practice of heavy overlaminates tying the parts to the hulls was inefficient. An alternative design was suggested, utilizing both a tougher adhesive system and a lighter overlaminate[17,18]. However, more study would need to be done to be comfortable with wholeheartedly recommending a major change in the attachment of such major structural members as stiffeners and bulkheads.

Repair applications of bonded composite joints appear to be reliable. The use of cold cure adhesives, once environmental degradation is accounted for, show promise[2]. This would allow for a major savings in operating costs due to the decreased equipment costs required to carry out the repair. The use of composites to repair non-composite structures is an interesting application. Early indications are that it shows promise, especially as the fatigue lives greater than the original structure have been indicated[3]. The effects of environmental degradation were not addressed, however. In service where a corrosive environment is encountered this could be a problem. Still, the advantage of being able to repair a metallic structure without drilling and riveting or welding is very real.

The use of adhesive bonded joints should continue to increase. More research into the longevity and fracture toughness of joints is an ongoing process. the use of toughened adhesives is an approach being used for the fracture toughness, with more ductile adhesives showing promise[10]. Still, many examples of laminated wooden structures such as hot-molded wooden sailing yachts are over thirty years old now and still holding up well. If these old adhesives are in good shape, continued development in both

adhesives and analysis will only enhance the potential for longer lived structures utilizing more examples of bonded joints.

Chapter 3

Experimental Work

3.1 The Current Work

This study explored the applications of two new tools to the examination of the fracture of adhesive joints in carbon fiber reinforced plastics. These are a video microscope (VM) and a confocal scanning laser microscope (CSLM). The video microscope is a light microscope that will record an image directly onto a conventional VHS tape, creating a real time record. With this tool, crack propagation can be recorded up to the point of final failure. Final failure occurs more rapidly than the camera is capable of recording. This machine is highly portable and has interchangeable lenses for greater versatility. The CSLM is capable of actually measuring a surface profile. The use of this ability to measure plastic deformation in the fractured adhesive surfaces was explored.

The joint configuration tested was that of a single lap joint. This configuration is the simplest to manufacture, and it is also the type that is most prone to peel stresses. These peel stresses are due to the couple created by the misalignment of the load paths, which results in a bending moment (Figure 3.1). While not desirable from the structural engineering standpoint, this configuration lent itself to more ready observation of the initiation and propagation of cracking. In addition, due to the simplicity of the joint design, it is often used in practice. As all of the lap and doubler joints, even the symmetrical ones such as the double doubler joint, have been found to have these peel

stresses, it should be possible to extrapolate the results from single lap joints to other, more complicated configurations.

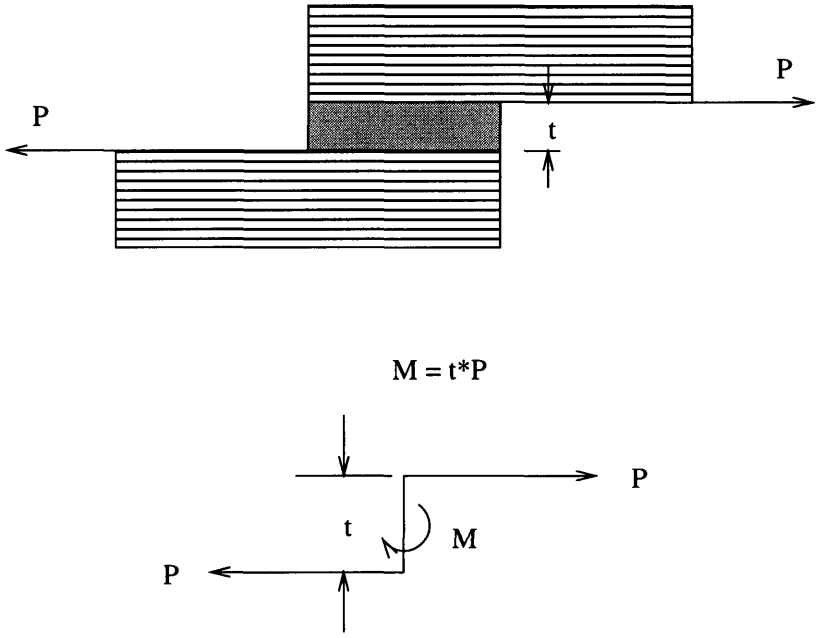

Figure 3.1: Moment due to misalignment of centroids

Three different adhesives were used for these experiments. There were two epoxies, which are relatively brittle, and a very ductile adhesive, a methacrylate ester. One epoxy, Gougeon 105 resin with a 205 hardener, was chosen as it is a commonly used adhesive system in the recreational boat building industry. It has a manufacturer's specified elongation to failure of 3%. The second epoxy, Hysol 9430, was chosen to represent a more "high tech" adhesive. This type of epoxy is more typically used in the aerospace industry, although it was used for the bonding of components in at least one America's Cup Class yacht built at Goetz Custom Sailboats for the 1995 America's Cup defense.It has a manufacturer's specified elongation to failure of 6%. The methacrylate ester adhesive was Plexus MA 550, which has a manufacturer's specified elongation of failure of 50-100%. This adhesive was chosen in order to compare the behavior of the joints when a very ductile adhesive was used, as compared to the relatively brittle epoxies.

Methacrylate esters are finding uses in the marine industry as they can bond many different materials, such as Lexan(tm) to FRP.

CFRP was chosen as the adherend laminate. This material, while not as common as glass fiber reinforced plastic (GFRP), is representative of the state of the art in adherend materials in the marine industry. It has been used for entire hulls of racing yachts, and is particularly for component applications where stiffness is a particularly important design parameter. Examples of these types of parts would be rudder stocks and sailing yacht spars. The samples consisted of seventeen plies of 153 grams per cubic centimeter unidirectional carbon, pre-impregnated with YLA RS-1 resin. The laminate had a $0^{o}/90^{o}$ orientation, with the 0^{o} plies on the exterior faces. This ply configuration is the simplest configuration that is likely to be used in an application. It was felt that a strictly unidirectional laminate was an unrealistic adherend configuration in terms of representing actual applications. The specimens were cured under a vacuum bag at a temperature of 100 C^{o} and atmospheric pressure. This resulted in a finished laminate thickness of approximately 1.7 mm. The 0^{o} axis was the long axis. The specimens were trimmed to a width of 50 mm and a length of 400 mm before adhesive bonding.

All of the samples were subjected to the same preparation procedure. This procedure consisted of machine cleaning the surface of the adherends with a Scotchbrite (tm) pad on a seven inch diameter sander/polisher. This was followed by an acetone wipe just prior to bonding to remove dust and any oils. The adhesives were mixed according to the manufacturers' directions. In the case of the Gougeon adhesive, colloidal silica was added to the adhesive in order to increase the viscosity to prevent the adhesive from running out of the joint before curing. This practice is commonly used in the boatbuilding industry [21, p.62].

The sample dimensions were duplicated as carefully as possible. The nominal dimensions were 50 mm width and 25 mm overlap. The individual samples were measured after assembly in order to calculate surface area and adhesive thickness. The finished sample length was approximately 700 mm in order to have the joint far away from any end effects created by the grips. To place the joints in more of a shear mode, shims were added to one side of each grip point in order to better align the samples in the grips of the test machine.

The samples were tested in a tensile test machine. The machine was a four post MPS Material Test System. The grips were hydraulically actuated, with an initial pressure of 400 psi, which was later increased to 600 psi. This was due to the lab's standard procedures; the maximum applied load allowed was initially 10000 lbf, but later was increased to 20000 lbf, for which the lab recommended grip pressures of 600 psi. The test was run in a stroke controlled mode, at a rate of 750 seconds/half inch. The sampling rate was 1 hz. The load data was measured with a load cell in line with the test machine piston, and collected with a Labview(tm) program, which incorporated an analog to digital converter. The data was collected on a Macintosh 2X computer into a Microsoft Excel spreadsheet. The output was calibrated to read in pounds force, not Newtons.

The video microscope was mounted on a table which allowed motion in the x and y axes. This table was in turn mounted upon a scissors jack which allowed motion in the z direction. The entire mounting arrangement was in turn clamped to a shelf attached between two legs of the test machine. The microscope was oriented to view the end of one side of the joint (figure 2.2). The video microscope was a Hirox model KH2200-MD2. The lens used was a Hirox model MX-2010Z, which is a 20X to 100X zoom lens.

Still pictures were taken from the video tape data with a Sony color video printer, model UP-3000. The laser microscope was a Lasertec model 1LM11.

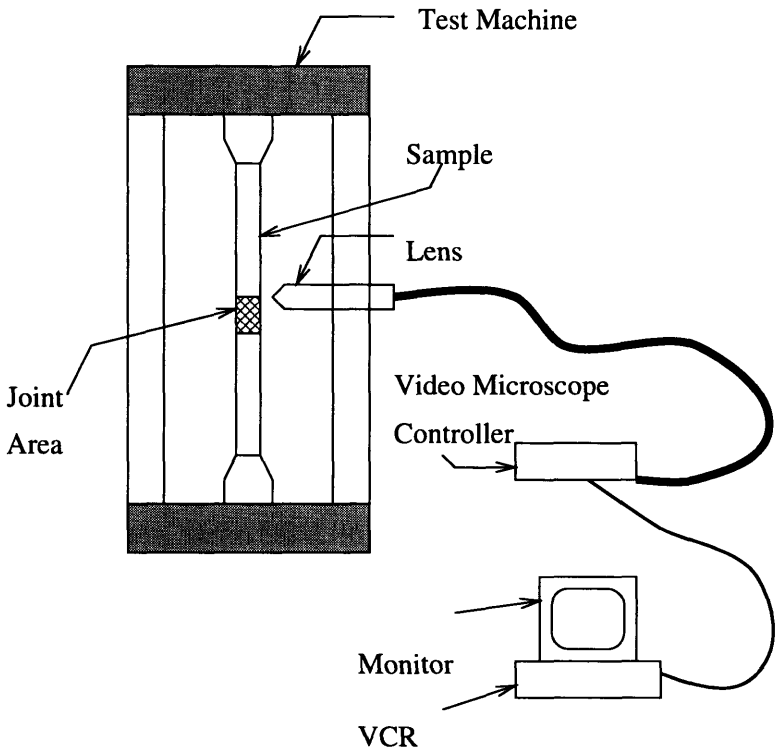

Figure 3.2: Test Setup

3.2 Specimen Specifications and Results

3.2.1 Hysol specimens.

The average adhesive thickness varied from 0.11 mm to 0.3 mm. The length of the overlap was 23.8 mm (.9375 in), for a surface area of 1190 mm^2. The specimens were observed from the side, with the lens set at 40X magnification. The spew fillet was not removed. These samples were labeled **h**.

Four of the five of the **h** samples showed a substantial amount of the joint failure to be interlaminar failure of one of the adherends, as opposed to cohesive, within the adhesive, failure. The one exception is believed to have been a defective batch of adhesive, as the sample failed with a dull thud and the failed surfaces felt greasy. Some yielding was observed on the load graph for all of the Hysol samples.

3.2.2 Plexus specimens:

actually the first tested. Their results were not analyzed, as the samples, labeled **a** for acetone solvent prepared and **d** for diatone solvent, were unfortunately not very consistent in their preparation, the overlaps were not always the same, and oftentimes there were gaps. These samples were useful to test the machine setup and practice with the video microscope. It was with these samples that the magnification was decided upon for the remainder of the tests. A magnification of approximately 40X on the monitor gave the best compromise between detail observation and a large enough field of view. The adhesive was Hysol EA 9430, the same as the five **h** samples. The glue line was generally more narrow. The load data was very linear for both types of surface treatments. The actual failure loads varied, but the linearity of the load versus time figures did not vary significantly. The behavior was very much a brittle type of behavior, very little plastic deformation was seen. The video microscope showed no crack formation until the sudden catastrophic failure. Previous studies have concluded that a high thickness ratio is desirable for a strong joint [14]. Certainly there was little yielding observed. The Hysol specimens prepared for this series of experiments had a thicker adhesive layer, as compared to the acetone and diatone samples, and the failure loads were lower, lending support to this conclusion. The adhesive batches were not the same however.

Chapter 4

Experimental Results

4.1 Video Data

The video's microscope ability to make a continuous record of an experiment allows an observer to review an experiment and compare the results of load data with the visual record. This is particularly useful for examining if an apparent yielding that is indicated by the load curve originates from deformation or cracking of the adherend or adhesive.

4.1.1 Hysol samples, general comments

The Hysol samples, with one exception, exhibited failure in the adherend itself. The one exception, **h4**, is likely to have been an imperfectly cured batch of adhesive. The specimen failed with a dull thud, as opposed to a sharp cracking sound of the other samples, and the surface of the failed adhesive felt greasy. For the other four, the adherend was observed to fail by delaminating, and the crack both propagated and opened. The crack failed at the interface between the outer 0^{o} ply and the adjoining 90^{o} ply. The initiation of the crack was actually outside of the actual joint area for at least one sample, **h2**, and at the end of the joint for the others.

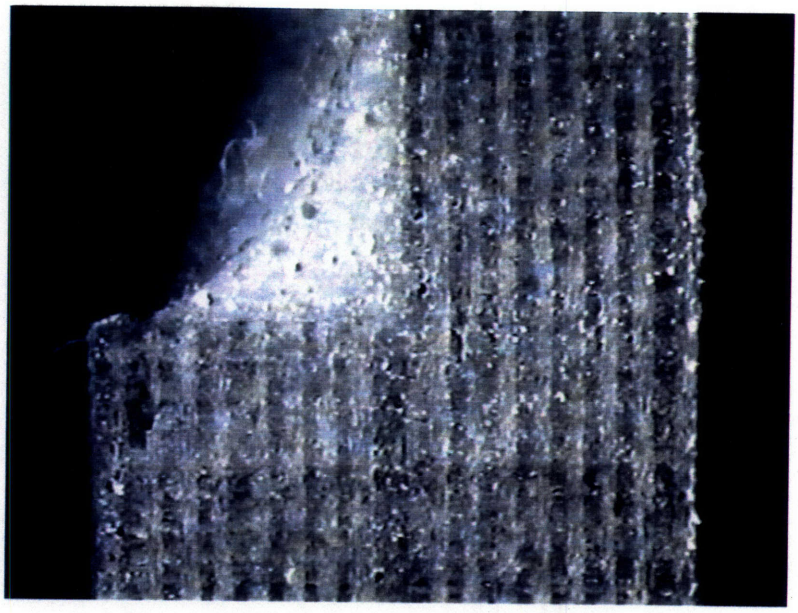

Figure 4.1: Typical Hysol Sample Before Testing

4.1.2 Plexus samples, general observations:

The Plexus samples showed deformation in the adhesive. This could be observed as a distortion of voids on the surface, and a distortion of marks created by the sanding process used to clean the edges for observation. These marks were normal to the plane of the joint. The distortion was entirely in the adhesive, originally indicated as deformations of voids or the sanding marks. As the displacement continued to increase, neighboring voids would distort and join with what appeared to be a ductile fracture. Failure would also occur at the adhesive-adherend interface, with a crack appearing and opening in what seemed to be Mode I failure. In at least one specimen, a crack at the adhesive-adherend interface rapidly cracked from one interface to the other in an approximately 45^{o} direction. This would indicate that the cracking changed from Mode I to Mode II, and then back to Mode I. While the overall fracture surface after failure appeared to be a shear mode, the video data showed that the bending moment created by the couple contributed to Mode I failure, as

cracks could be seen to be opening in a direction normal to the applied load, with the crack extension parallel to the applied load.

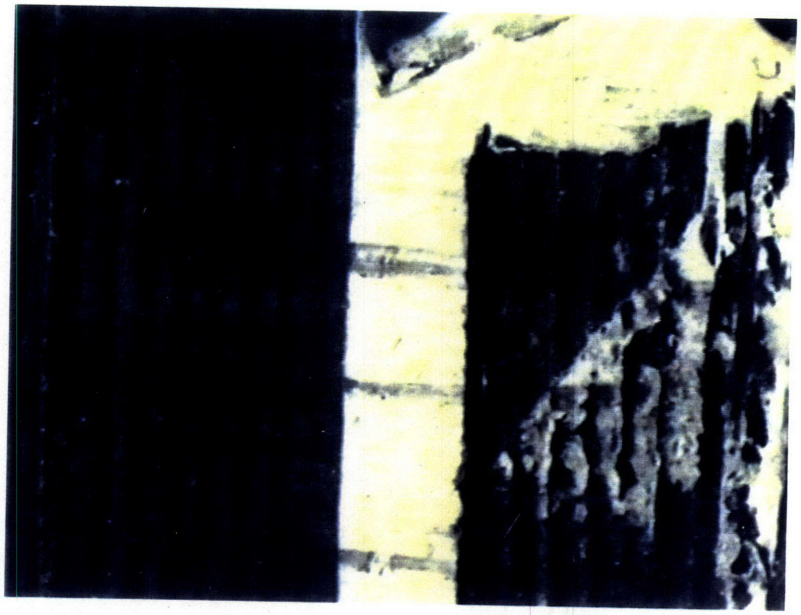

Figure 4.2: Typical Plexus Sample Before Testing

4.1.3 Gougeon samples, general observations:

These samples had the lowest failure loads. The load increase was very linear. These specimens exhibited no visible yielding, and they were the most consistent in failure load and mode. The failure was always in adhesion between the adhesive and the adherend, and very brittle; no cracking of the adhesive or delamination of the adherend was observed prior to the onset of sudden failure. There was some slight fiber transfer observed on the fracture surface after failure.

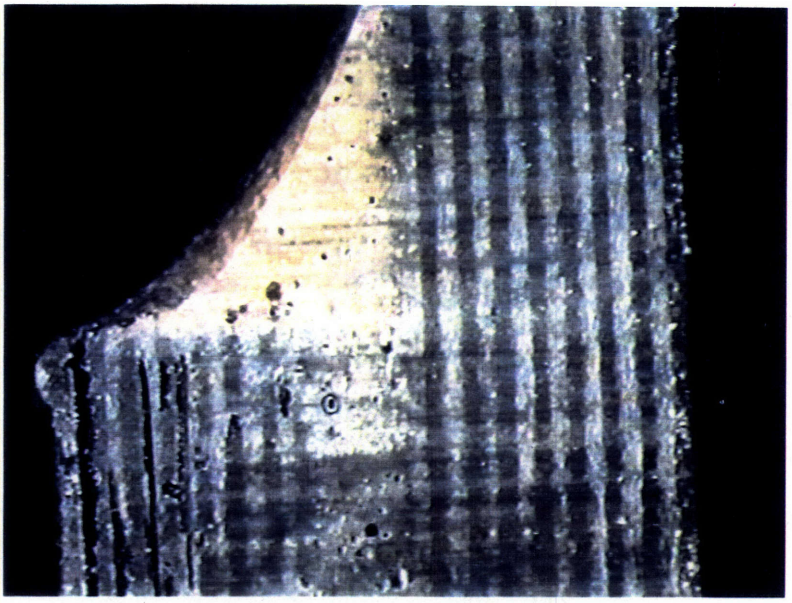

Figure 4.3: Typical Gougeon Sample Before Testing

4.2 Correlation of Load and Video Data

The video microscope was the most useful for the study of the failure of the Hysol and Plexus samples. Both types of samples exhibited some yielding in their load behavior. The continuous record of the videotape allowed the visual data to be compared with the load data. The Gougeon samples, due to their failure mode, were not as suited to the use of the video microscope. This is due to the rapid failure of the Gougeon samples in adhesion; no visible deformation or cracking was recorded up to the point of sudden failure. The load graphs also exhibited a very linear behavior right up to the failure of the sample.

The load versus time graphs of the samples were reviewed. Representative samples of each adhesive type were selected for closer examination. The areas of interest were the non-linear portions of the graph, as it is at this point when some type of cracking or deformation of the adhesive or adherends is expected to occur.

4.2.1 Hysol Samples:

These samples exhibited a primarily linear load behavior for the majority of the test (see figures 3.4, 3.11). Towards the end of the tests, all of these samples exhibited a non-linear behavior of the load data. Sample **h2** and sample **h5** exhibited the most extensive cracking prior to failure. This cracking was within the plies of the adherend, between the 0^o and the 90^o plies adjacent to the joint. The linear portion of the load data ran from 5 seconds to approximately 70 seconds, with the non-linear portion occurring from 70 seconds to failure, which occurred at about 105 seconds for both of these samples.

4.2.2 Sample **h2**

Cracking was first observed at 55 seconds, and it occurred outside of the joint area (see figure 3.6). Sample **h2** had a relatively large spew fillet, and cracking can be seen to be occurring beyond the spew fillet (see fig. 3.7). It is not until 75 seconds (see fig. 3.8) that the crack reaches the end of the joint. From then until failure, the crack continues to progress under the joint until final failure (see figs. 3.9, 3.10). Opening of the cracking can also be observed, particularly towards the end of the test (see figs. 3.9,3.10). This opening of the crack, in a direction normal to the applied load, is indicative of Mode I failure.

4.2.3 Sample **h5**

Cracking in this case was first observed at 75 seconds (see fig. 3.14). In a similar fashion to sample **h2**, the crack initially occurred outside of the joint (see fig. 3.14). At 95 seconds, the crack had lengthened slightly, and also opened (see fig 3.15). At 100 seconds, the crack had opened considerably under the end of the joint, and was also lengthening rapidly (see fig. 3.16).

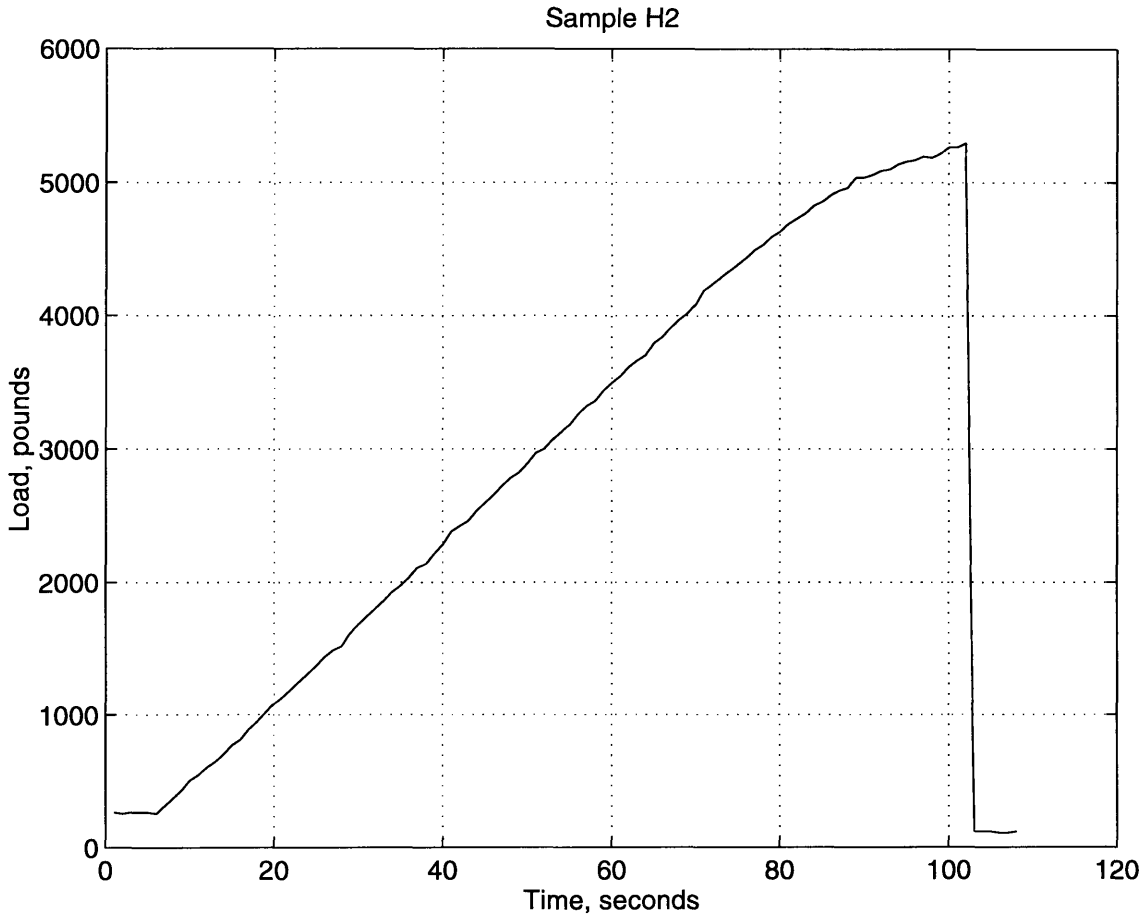

Figure 4.4: Hysol Sample **h2** Load vs. Time Graph

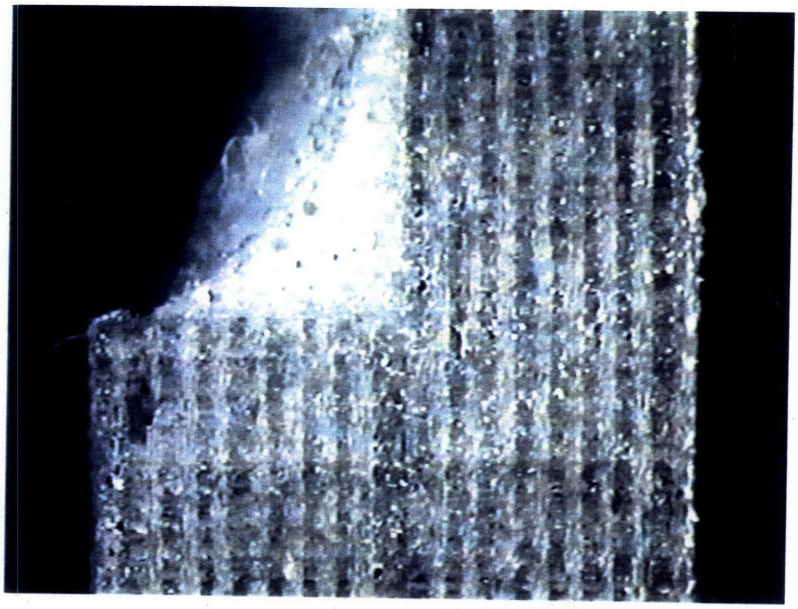

Figure 4.5: h2, Start of Test

This is the sample before loading is applied. Note that the spew fillet is relatively large, extending out of the field of view towards the top of the image. It is important to note that there are no existing cracks under the spew fillet or within the joint area itself.

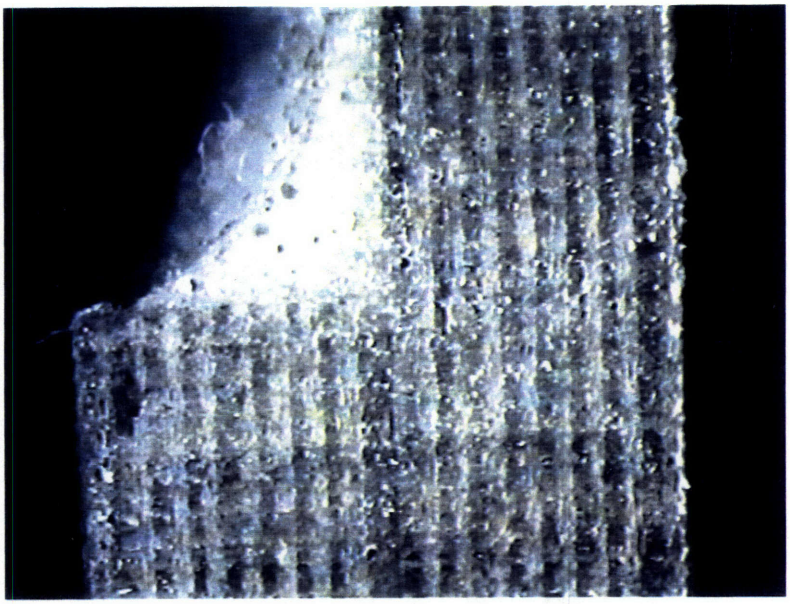

Figure 4.6: h2, 55 seconds

At this time, it can be seen that cracking has been initiated. What is interesting is that the crack is actually originating outside of the actual joint area. The crack actually extends out of the picture towards the top, away from the immediate joint area.

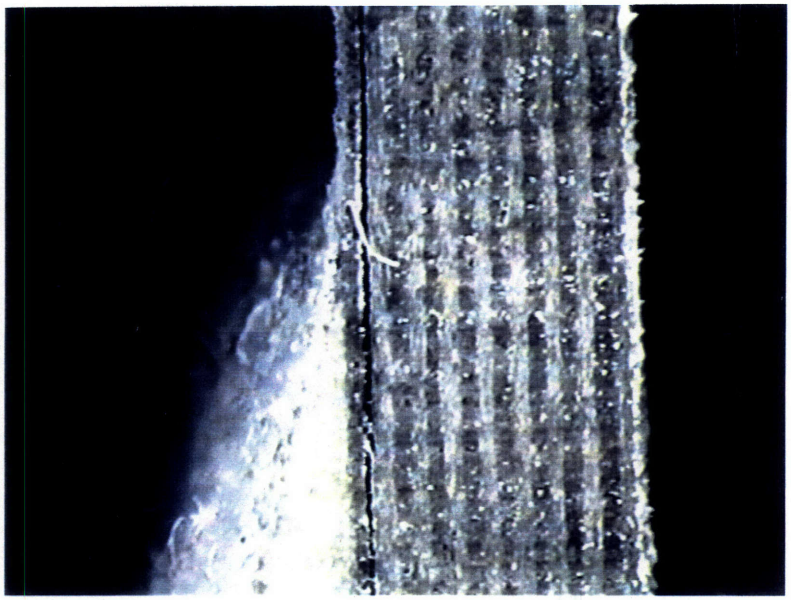

Figure 4.7: h2, 65 seconds

In this image, the video microscope has been raised to view the crack beyond the joint. The crack extends beyond the spew fillet, and the opening is greatest at the end of the spew fillet, which can be seen approximately one third of the way from the top of the image. It can be seen that the crack is lengthening in the direction of the applied load, but is opening in a direction normal to the applied load. Referring back to the load graph, figure 4.4, the load increase is still basically linear.

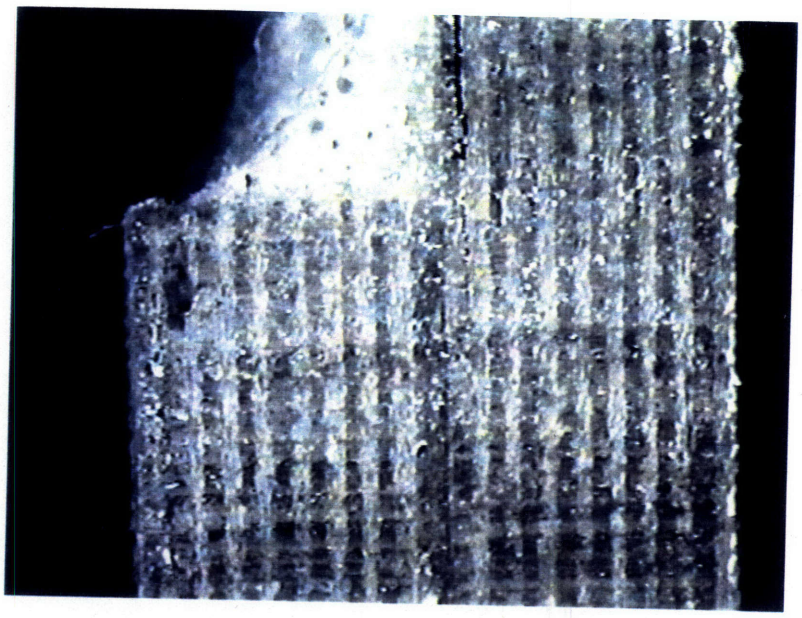

Figure 4.8: h2, 75 seconds

At this point, the crack has just reached the end of the joint. It has not lengthened much as compared with figure 4.6, 50 seconds, but the opening displacement is greater. At this point the load graph is beginning to exhibit a non-linear load increase.

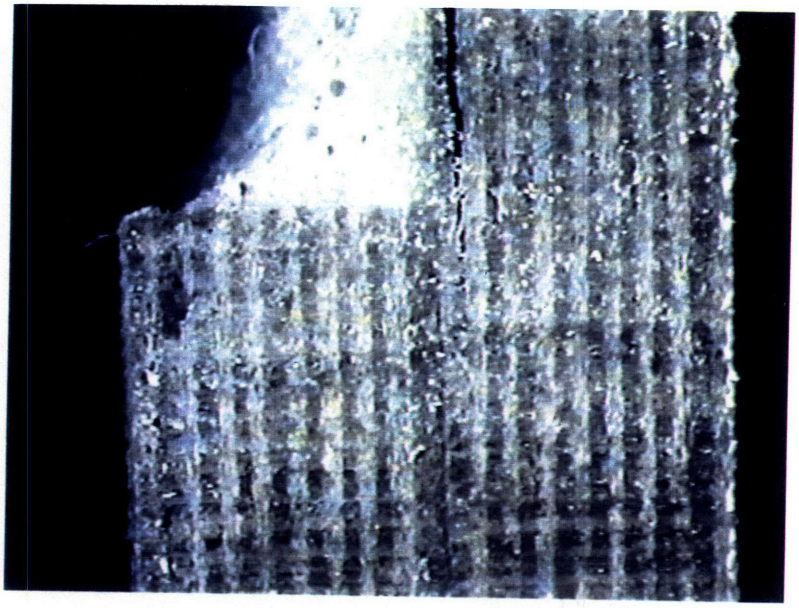

Figure 4.9: h2, 85 seconds

The crack has now distinctly opened, and can be seen to be progressing actually under the joint. The opening displacement is approximately twice the displacement in figure 4.8, 75 seconds. Note that the opening of the crack is increasing farther from the joint.

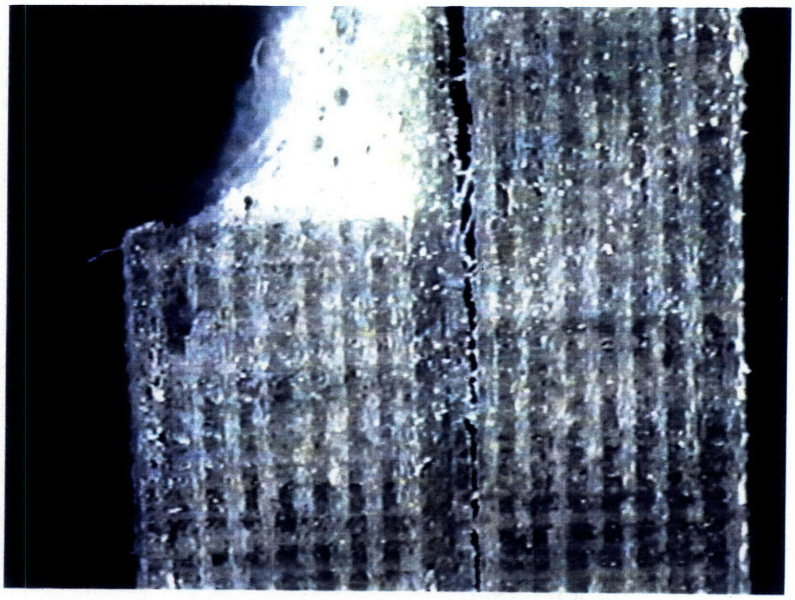

Figure 4.10: h2, 95 seconds

Here the crack is progressing under the joint at an increasing rate. An interesting observation is the much greater opening of the crack just outside of the joint area. This supports the prediction of peel stresses, and the greater opening outside of the joint would be due to the much lower stiffness.

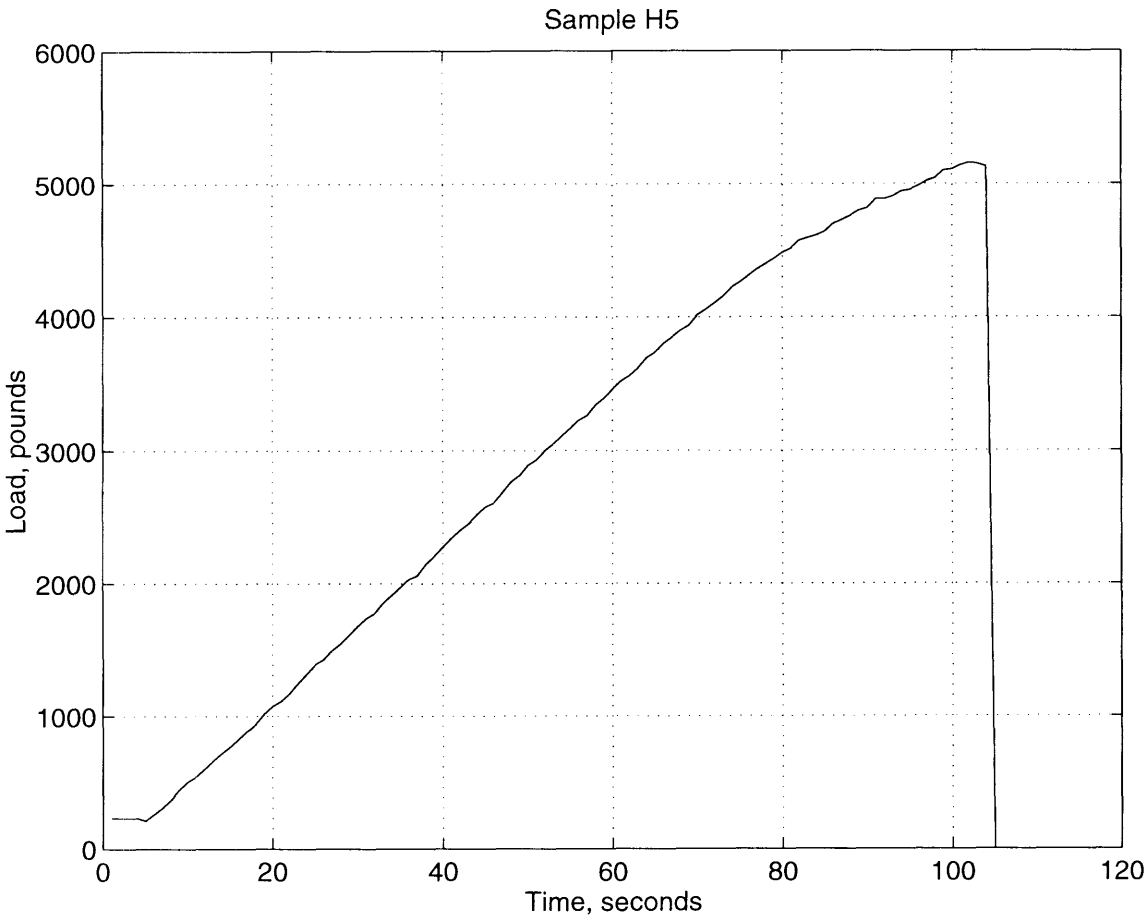

Figure 4.11: Hysol Sample **h5** Load vs. Time Graph

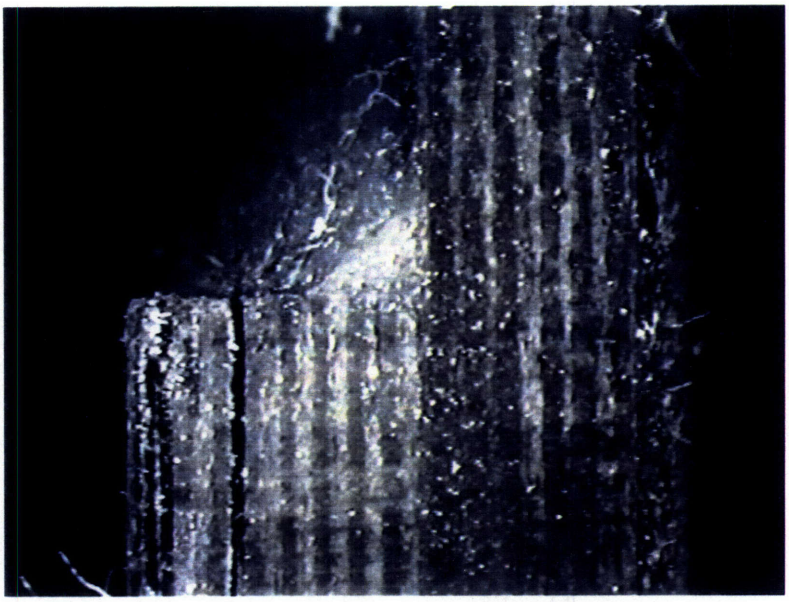

Figure 4.12: h5, Start of test

This is the sample at the beginning of the test, prior to any loading being applied. There are no existing cracks in the joint area, although a crack does exist in the adherend at the left side of the picture. This crack was the result of the cutting operation when trimming the strips to length.

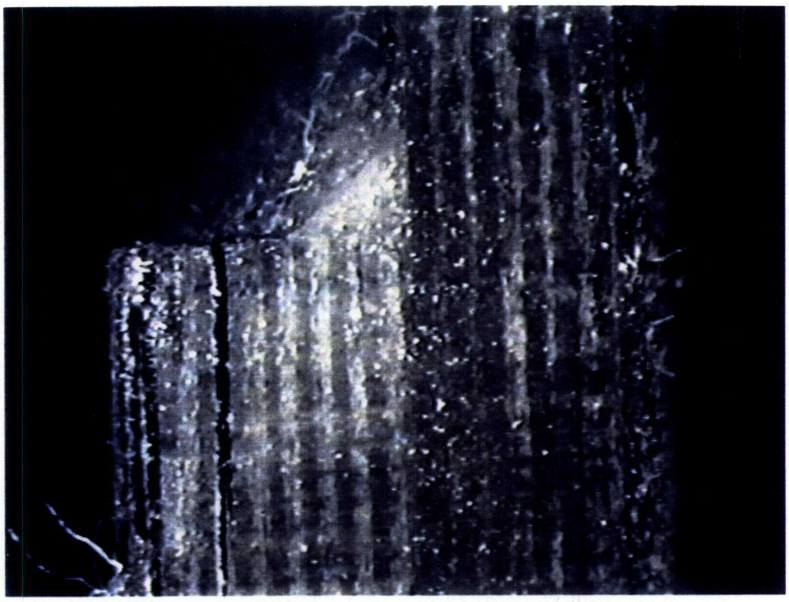

Figure 4.13: h5, 50 seconds

At this time, no cracking can be observed. The load increase, see figure 4.11, is still linear.

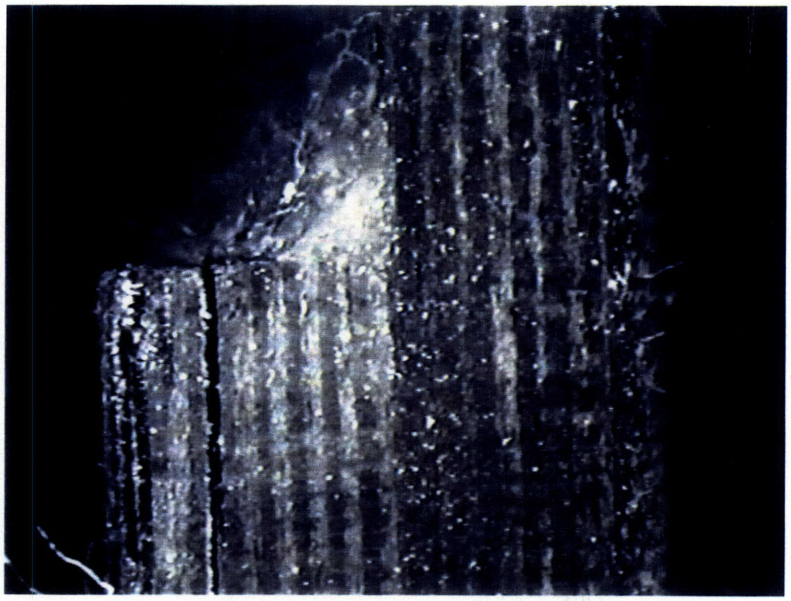

Figure 4.14: h5, 75 seconds

The very beginnings of a crack can be observed at this point. The crack is occurring underneath the end of the joint, in the middle of the image. The load increase in figure 4.11 shows the beginnings of a non-linear behavior at this time.

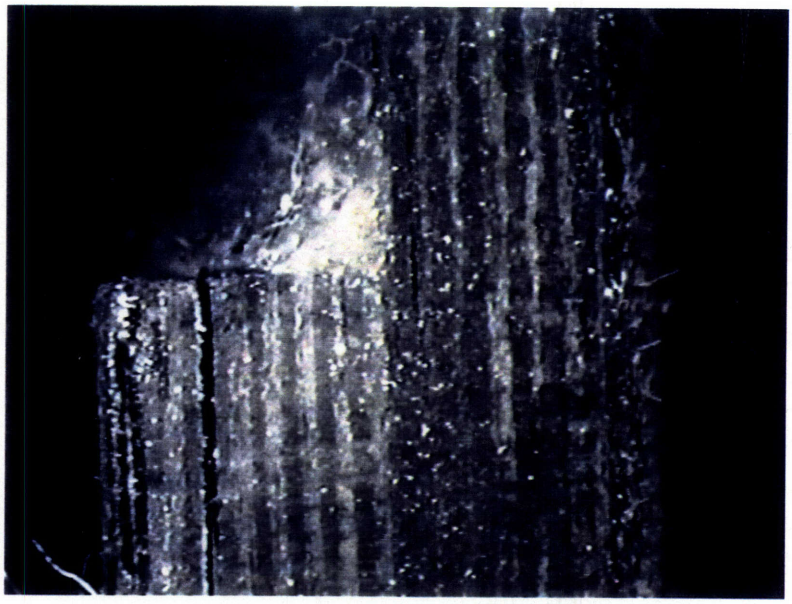

Figure 4.15: h5, 85 seconds

The crack is becoming more visible. At this point, the load increase graph shows an increasingly non-linear behavior.

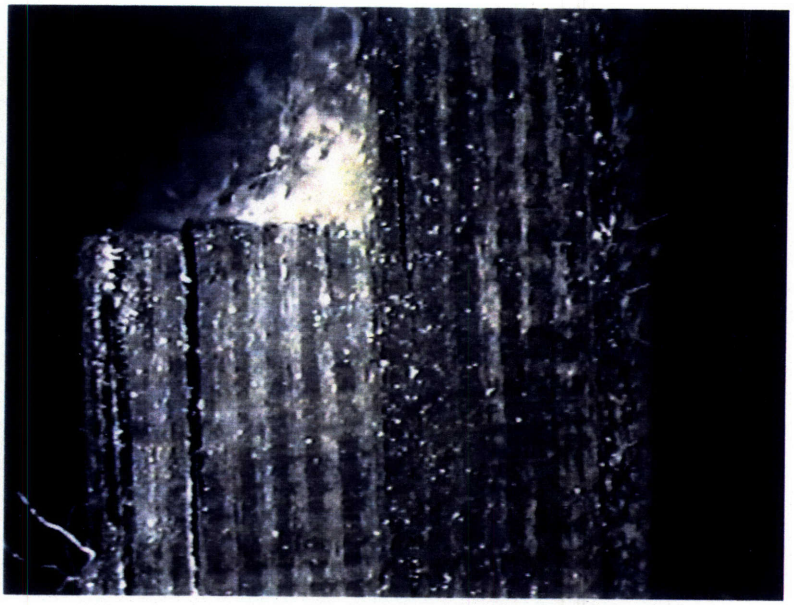

Figure 4.16: h5, 95 seconds

The crack has now become distinct. In a similar manner to the behavior of the crack in sample **h2**, the crack is exhibiting the majority of the opening beyond the end of the joint. Again, this supports the prediction of peel stresses concentrated at the end of the joint.

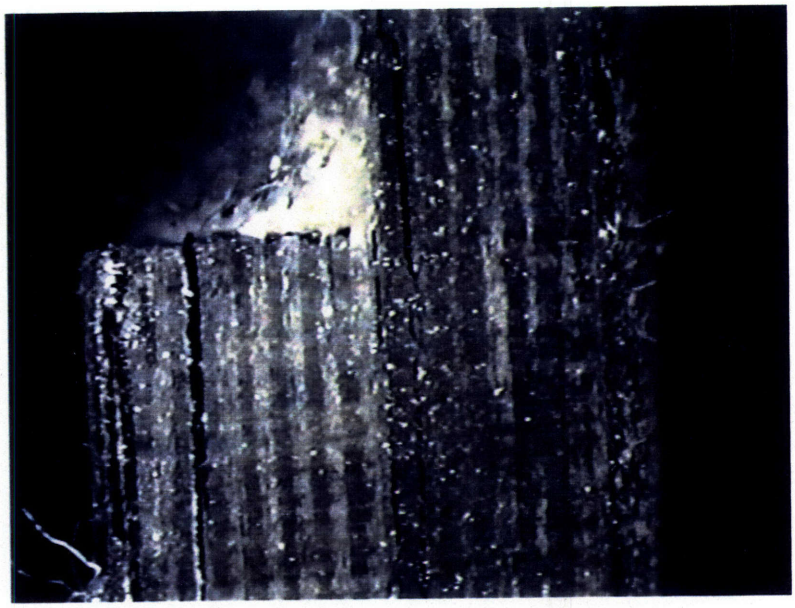

Figure 4.17: h5, 100 seconds

The crack is now rapidly propagating under the joint. However, the greatest opening displacement is beyond the ends of the joint. At the top of the image, fiber failure appears to have occurred, as can be seen by the distinct jog in the crack path

4.2.4 Plexus samples

These samples exhibited a ductile behavior in their tests. This would be expected from the specified elongation to failure. Samples **p1**, **p4**, and **p5** all exhibited a non-linear tendency at low loads, compared to the Hysol samples. There was also a distinct flattening, or plateau, exhibited in the region of the graph before failure. The video data showed the distortion of the adhesive and opening of cracks and voids clearly, corresponding to a combination of failure modes. The adhesive could be seen to be

distorting, which would be Mode II behavior, and cracks could also be seen to be opening, which is characteristic of Mode I failure.

4.2.5 Sample **p1**

Sample **p1** showed the combination of failure modes. Mode II sliding can be seen in the distortion of a scribe mark and sanding marks after 60 seconds (see fig. 4.20), as compared to the initial state (see fig. 4.19). At 90 seconds, the adhesive has cracked at the end of the joint, and the crack can be seen to be opening (see fig. 4.21). After 110 seconds, the adhesive has continued to open, which is Mode I, but Mode II failure is also occurring, as can be seen in the distinct mismatch of the scribe marks (see fig. 4.22).

4.2.6 Sample **p4**

Sample **p4** is a clear demonstration of the combined modes of failure. Mode II distortion was observed first, which can be seen in the distortion of sanding marks near the adhesive-adherend interface after 45 seconds (see fig. 4.24). After 55 seconds, a pre-existing void can be seen to distort, and the beginnings of a crack can be observed on the opposite side of the joint (see fig. 4.25). After 75 seconds, this crack can be clearly seen to be opening, which is Mode I behavior, and Mode II distortion is evident by the distortion of the sanding marks (see fig. 4.26). At 85 seconds, a crack has propagated across the adhesive, linking the void and the end of the crack (see fig 4.27). After 95 seconds, the crack is progressing along the adhesive-adherend interface, and some of the Mode II distortion has been relieved where failure has already occurred, as can be seen by the straightening of the sanding marks (see fig. 4.28).

4.2.7 Plexus sample **p5**

This sample showed Mode II distortion of the adhesive very clearly. Distinct marks can be seen across the adhesive at the beginning of the test (see fig. 4.30). After 50 seconds, distortion of these marks is clearly evident (see fig. 4.31). After 80 seconds, the beginnings of interlaminar failure in the adherend can be seen (see fig. 4.33). At 90

seconds this crack is more evident (see fig. 4.33). At 110 seconds, the crack is clear, and recovery of some of the Mode II distortion can be seen where the crack has occurred. The sanding marks have straightened where the crack has opened, but there is still Mode II distortion at the crack tip (see fig. 4.34). At 110 seconds the crack is opening and progressing at an increasing rate (see fig. 4.36).

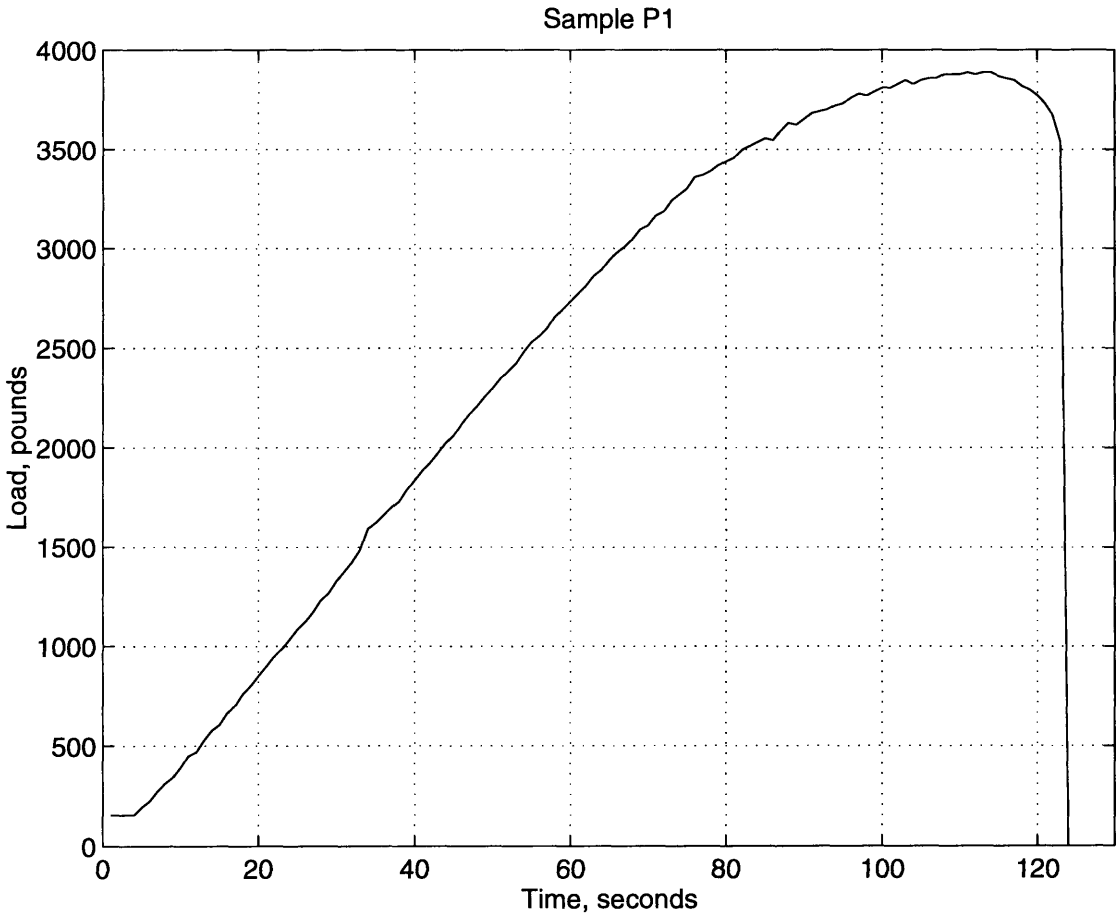

Figure 4.18: Plexus sample **p1** Load vs. Time Graph

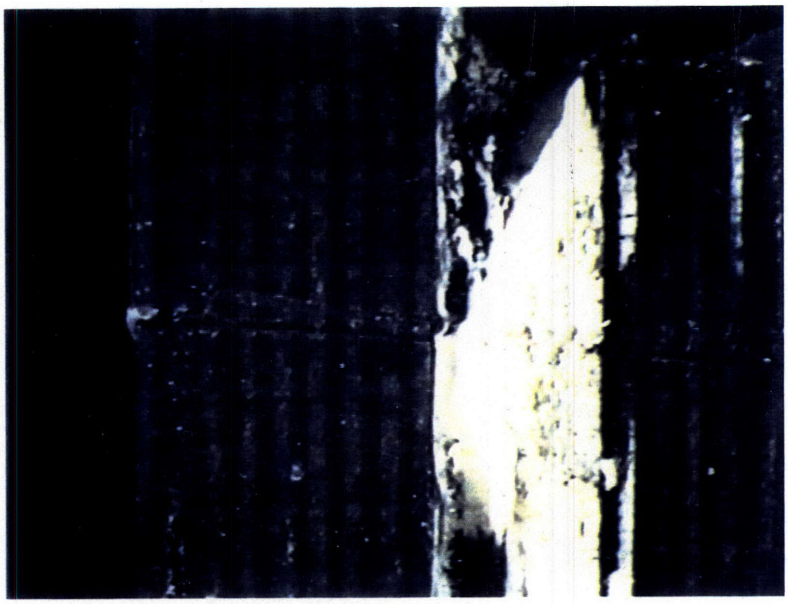

Figure 4.19: p1, start of test

This is sample p1 at the beginning of testing, with no significant tensile loading. There is a reference mark scribed across the joint, it can be seen in the approximate middle of the image. There is an existing flaw in the edge of the adhesive, the joint area is not completely filled with adhesive, this can be seen at the top of the image.

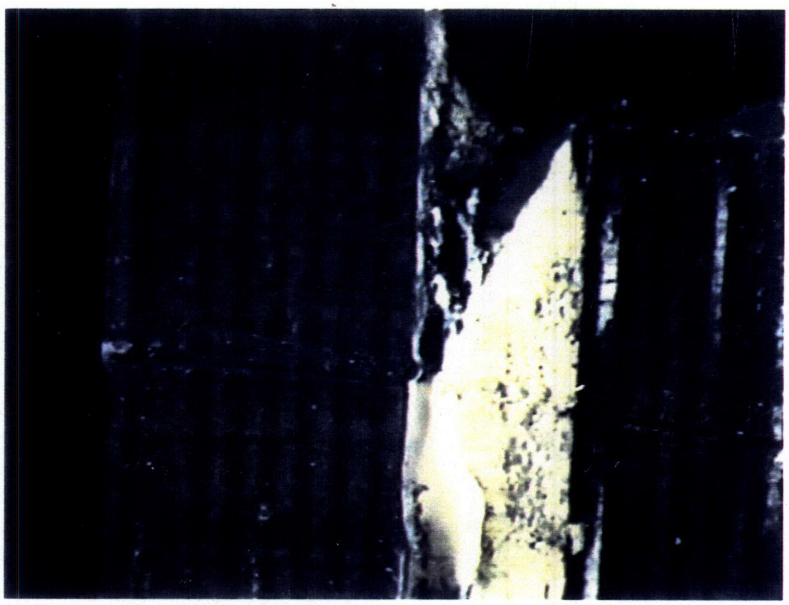

Figure 4.20: p1, 60 seconds

This image is taken at 60 seconds. As can be seen in figure 4.18, the load increase has just begun to exhibit a non-linear behavior. It can be seen that the adhesive has begun to distort in a Mode II manner, the scribed reference mark is no longer in a straight line.

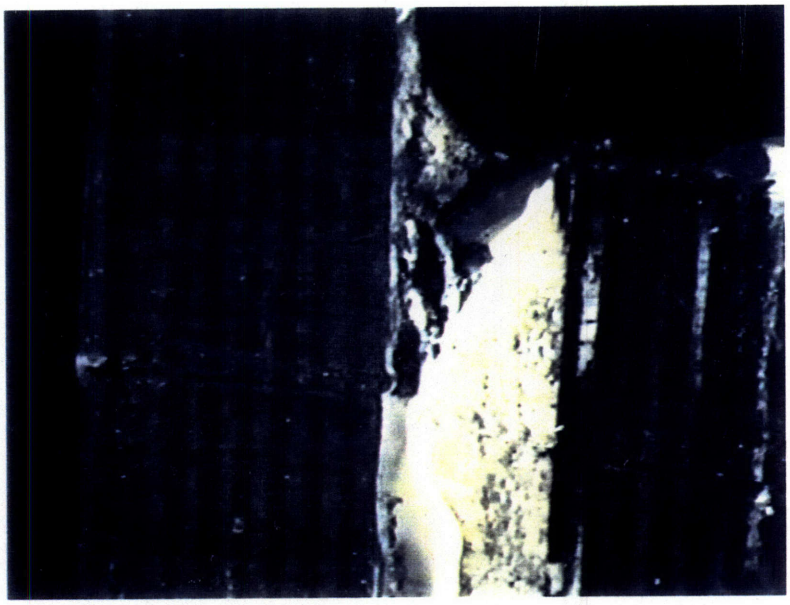

Figure 4.21: p1, 90 seconds

The Mode II distortion is evident here when examining the reference mark and the sanding marks in the adhesive. Mode I failure can also be observed in the adhesive originating from the end of the flaw in the edge of the adhesive.

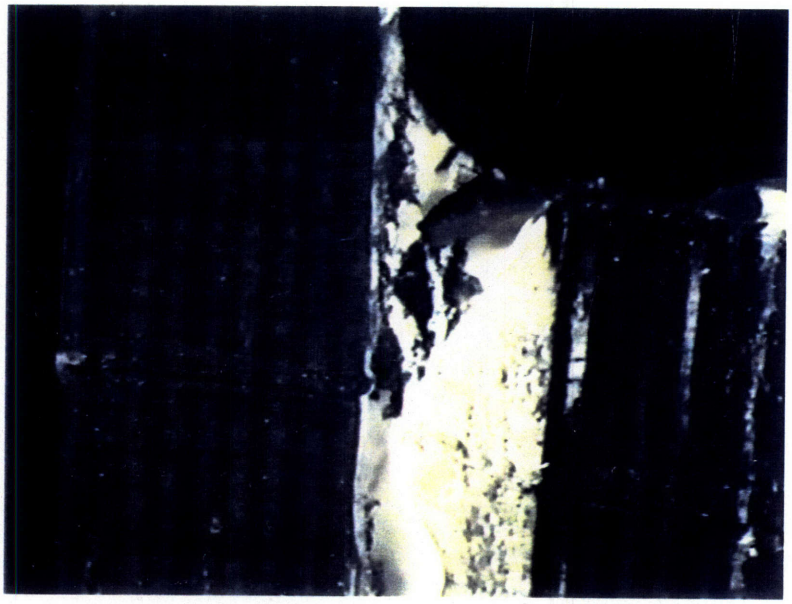

Figure 4.22: p1, 110 seconds

Mode I failure is continuing, and a large amount of distortion in the Mode II direction can also be observed. The Mode II failure is exhibited both by the distortion of the sanding marks and the extreme mismatch of the reference mark.

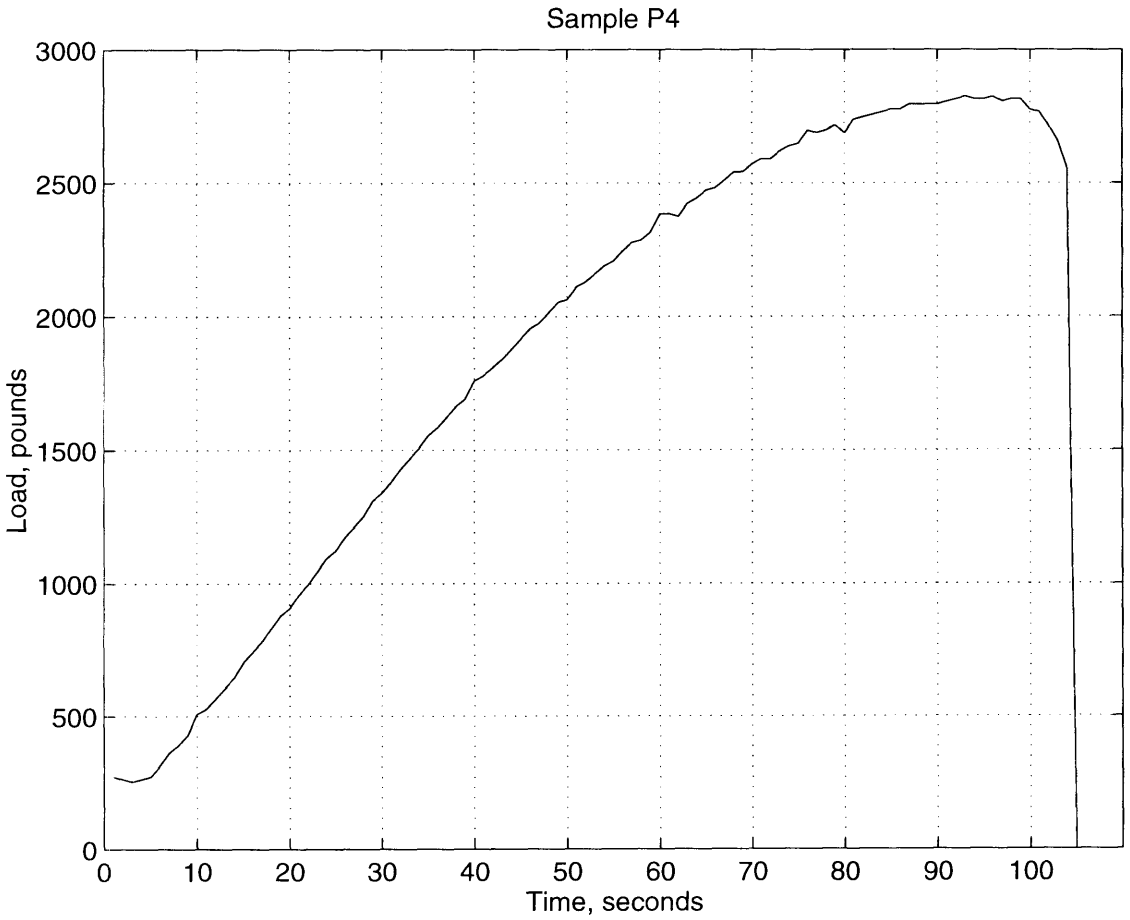

Figure 4.23: Plexus sample **p4**, Load vs. Time Graph

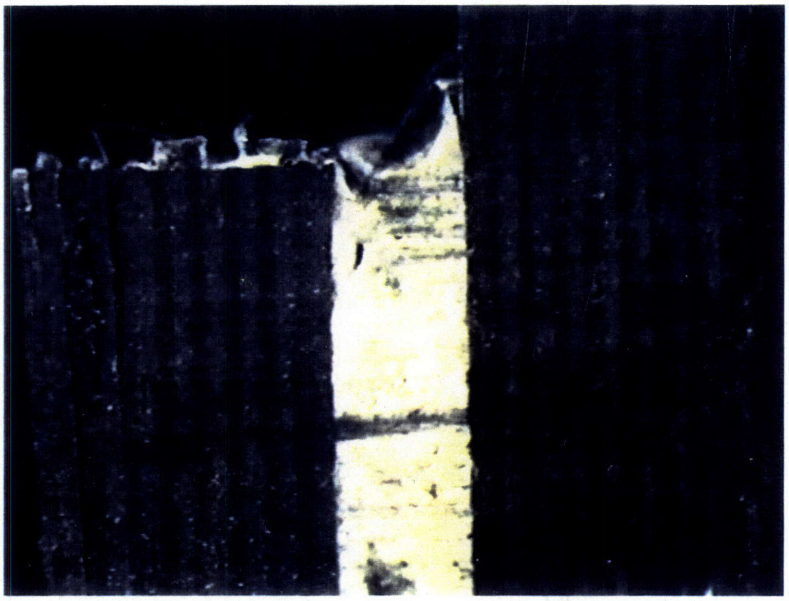

Figure 4.24: p4, start of test

This image shows the sample at the beginning of the test. Note the reference mark scratched across the joint, which has been highlighted across the adhesive with pencil. There is an existing void near the upper left edge of the joint. At the upper right edge of the joint the adhesive can be seen to be lifting slightly. These all were existing before loading of any significant amount occurred.

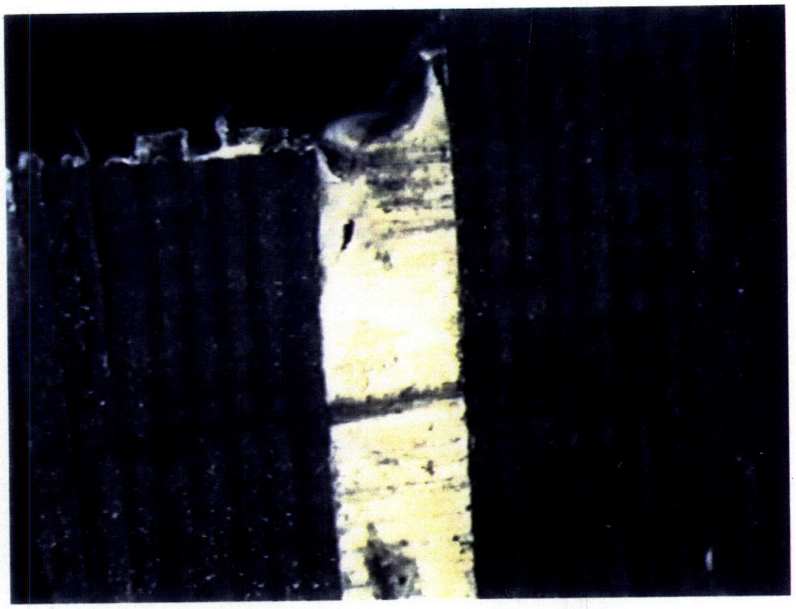

Figure 4.25: p4, 45 seconds

At this time, the void can be seen to be distorting. In addition, the reference mark shows Mode II movement of the joint. Figure 4.23 shows that the load data is beginning to exhibit a non-linear behavior at this time.

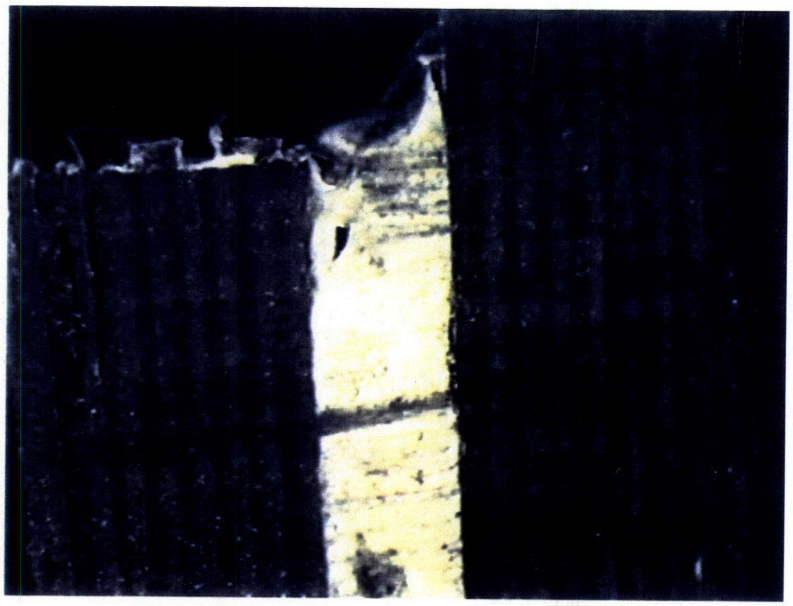

Figure 4.26: p4, 55 seconds

The void is much more severely distorting. The pre-existing curled area in the upper right is curling more. There is a crack forming along the adhesive-adherend interface at the right end of the pencil reference mark. This crack is opening in a Mode I fashion.

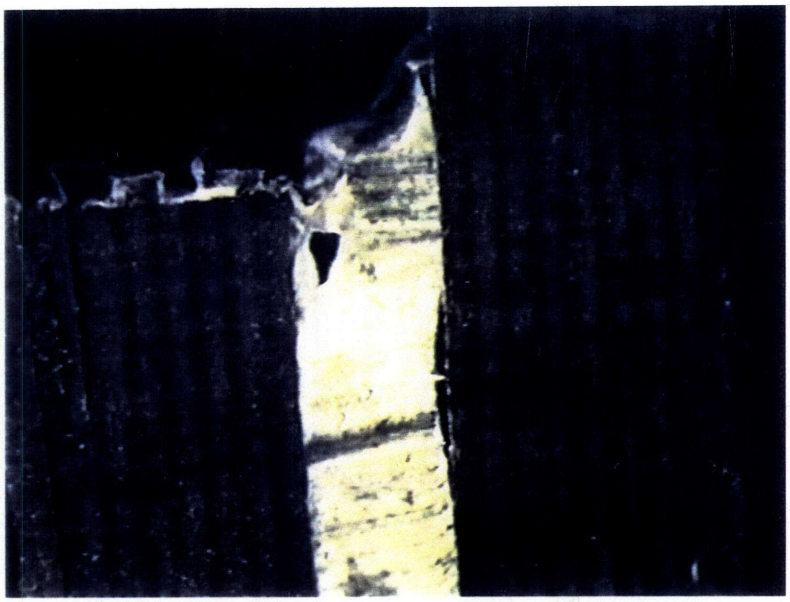

Figure 4.27: p4, 75 seconds

The void has become extremely distorted and enlarged. The crack formed at the right end of the reference mark has lengthened slightly, but opened considerably, indicating the presence of peel stresses at the end of the joint

Figure 4.28: p4, 85 seconds

At this time, a crack has propagated across the joint. This crack has linked the void and the upper end of the crack on the right side of the joint. It propagated at an angle across the joint, which would indicate some shearing stress.

Figure 4.29: p4, 95 seconds

This is an interesting image. The microscope has been lowered slightly to observe the crack tip progression. There has clearly been Mode II movement of the adherends, which can be seen by the mismatch in the reference marks and the widening transverse gap at the top of the image. That there are also peel stresses present can be seen by the wider end of the crack at the top, making a tall, narrow v along the right side of the joint. There has been some elastic recovery of the adhesive where this crack has propagated. This can be seen by the relative straightening of the transverse sanding marks in the middle of the image as compared to the distorted sanding marks across the joint at the bottom of the image.

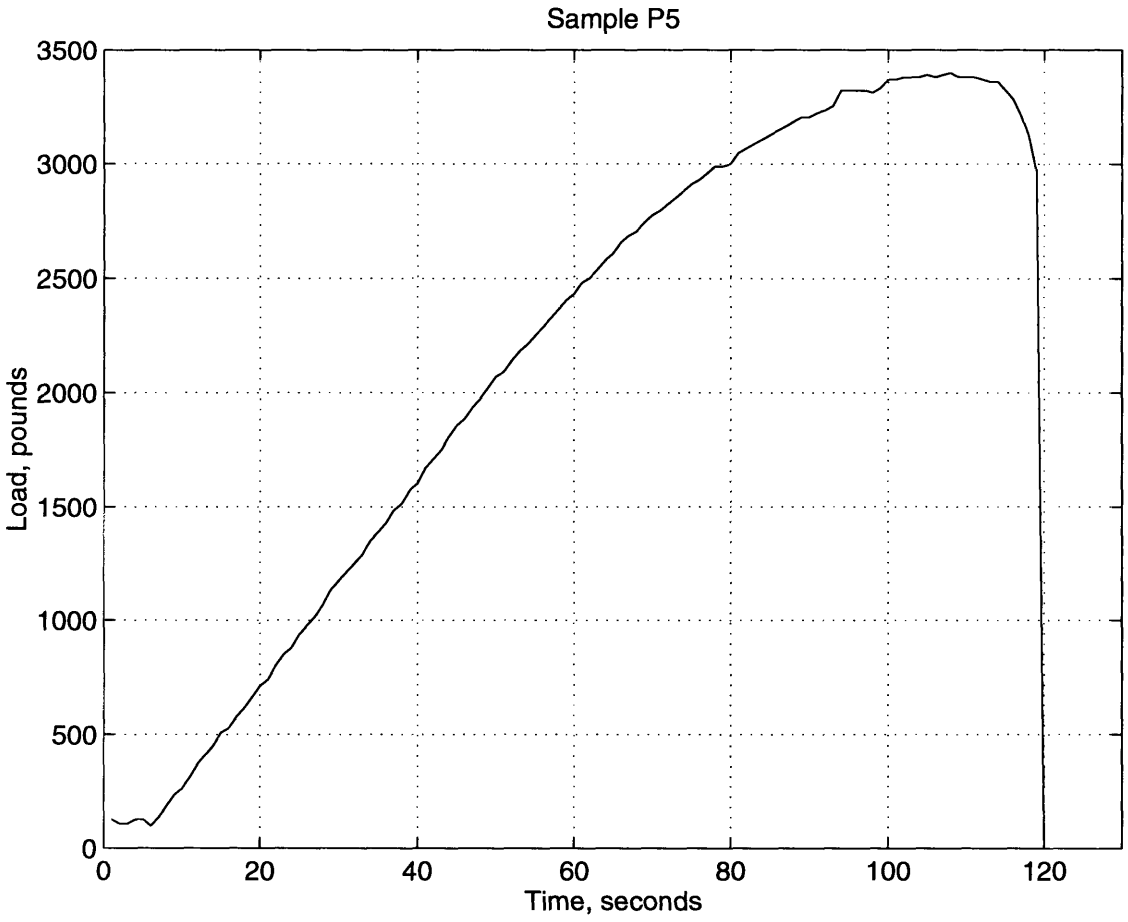

Figure 4.30: Plexus sample **p5**, Load vs. Time Graph

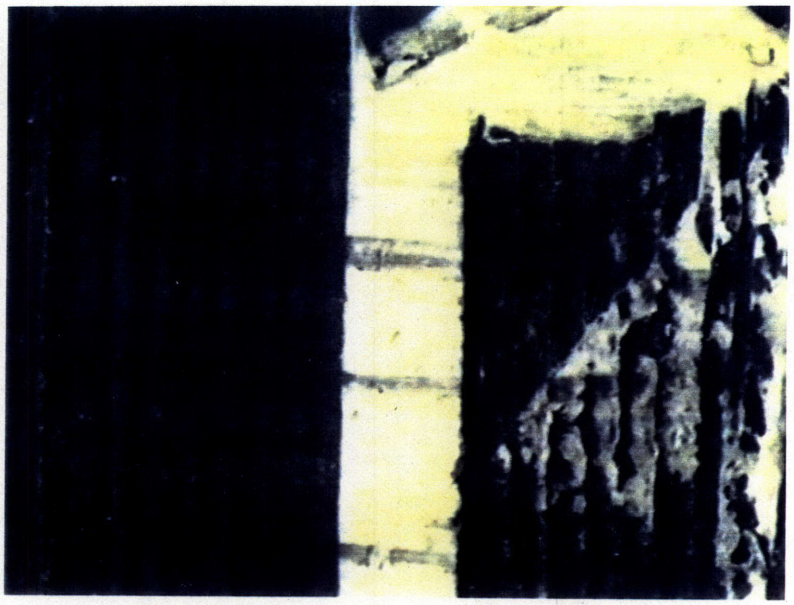

Figure 4.31: p5, Start of test

This sample has several reference marks across the edge of the joint. There are no significant voids, although the end of the joint exhibits a slight undercut.

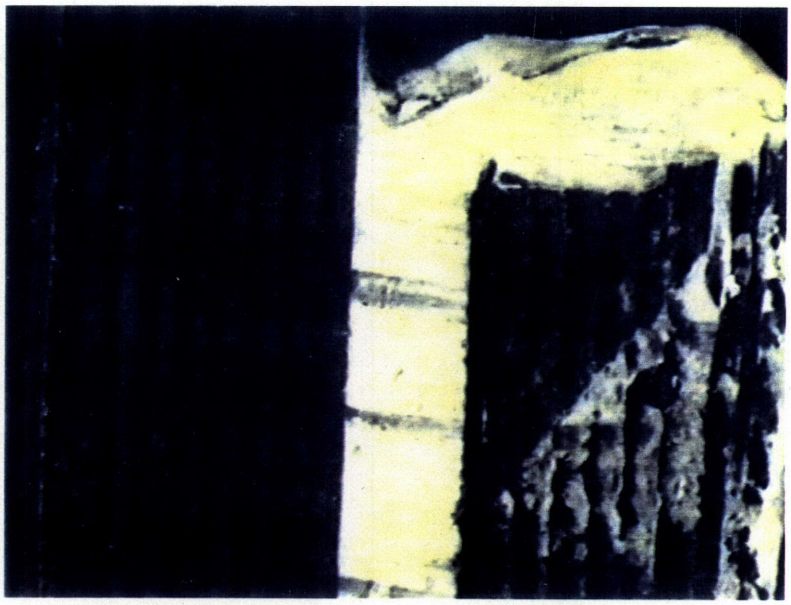

Figure 4.32: p5, 50 seconds

This image shows only Mode II motion at this point. This can be clearly seen by the distortion of the reference marks across the joint. The microscope has been lowered slightly as compared to figure 4.31.

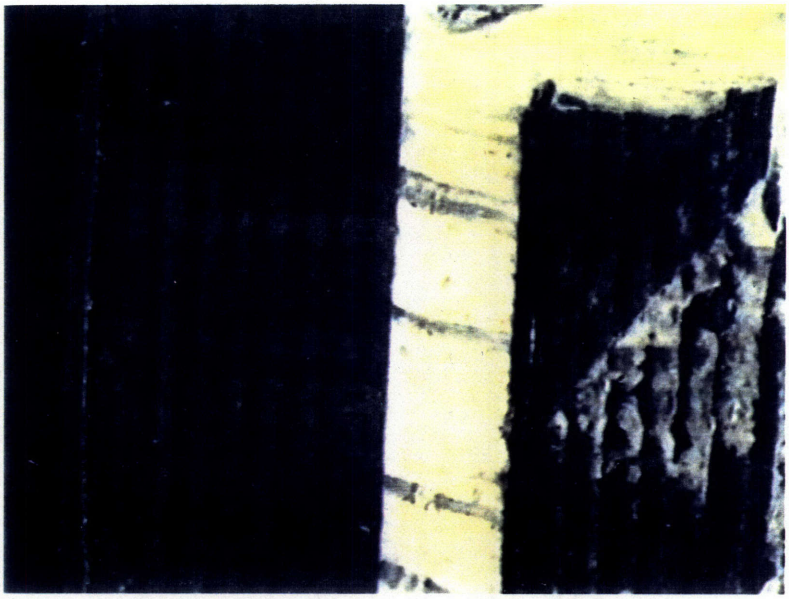

Figure 4.33: p5, 80 seconds

This image continues to show Mode II movement. There is a crack forming between the first 0^{o} and the first 90^{o} plies just to the right of the adhesive.

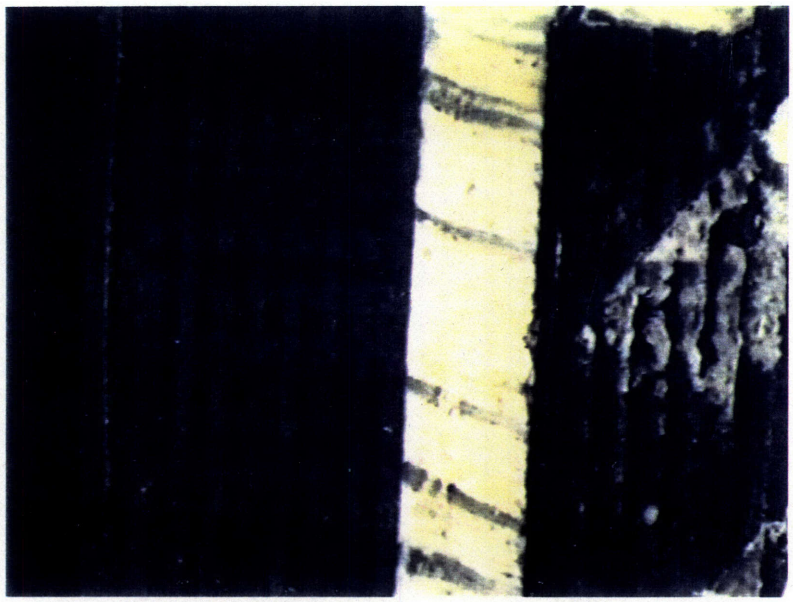

Figure 4.34: p5, 90 seconds

In this image it can be seen that the crack between the 0^{o} and the 90^{o} plies is continuing to open. Mode I failure of the adhesive has not begun to occur.

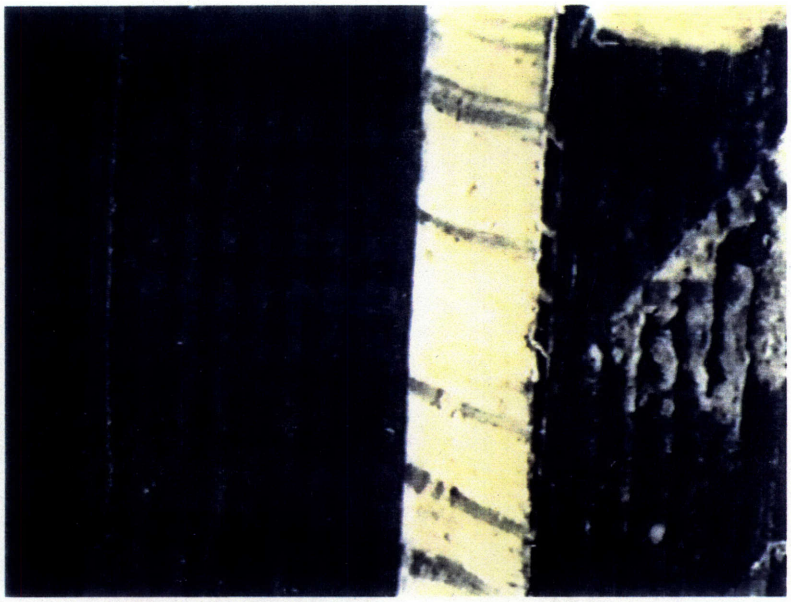

Figure 4.35: p5, 100 seconds

Mode I failure is now occurring along the right side of the joint along the adhesive-adherend interface and the interlaminar crack in figure 4.33 has closed up. The elastic recovery of the adhesive can be seen by the straightening of the reference marks at the top of the image as compared with the much more distorted reference marks at the bottom of the image.

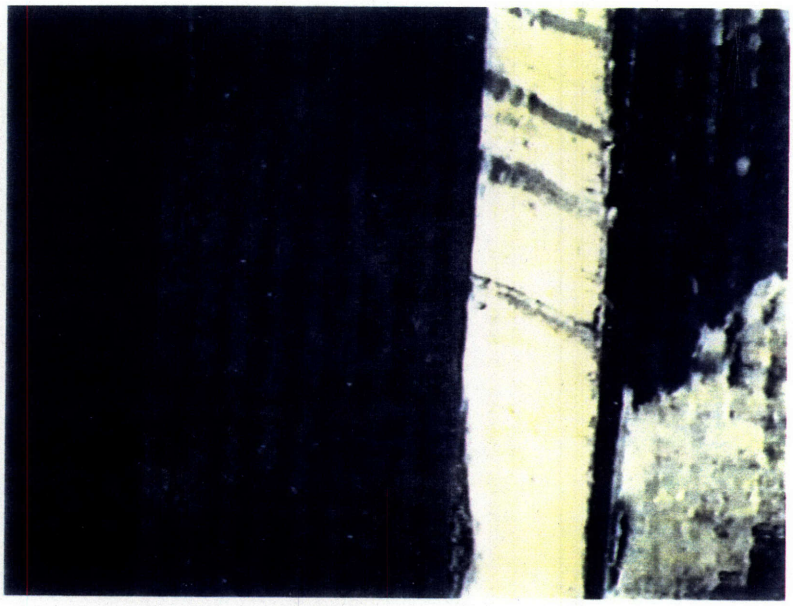

Figure 4.36: p5, 110 seconds

For this image, the microscope has been lowered to follow the crack tip. The crack is continuing to open in a Mode I fashion, and the crack tip is progressing down the adhesive adherend interface. At the lower left part of the image, another crack can be seen to be forming.At this point the load increase is beginning to flatten considerably, as can be seen in figure 4.30.

4.3 Laser Microscope Results

The laser microscope was used in an attempt to measure the plastic deformation of the adhesive surfaces after fracture. A Plexus sample was selected for this. The profiles of the mating surfaces at the same point were measured. The samples were carefully aligned, in order to ensure that the same point was, indeed, being measured. A profile was measured, but no correlation between the two surfaces could be observed (see figures 4.36, 4.37).

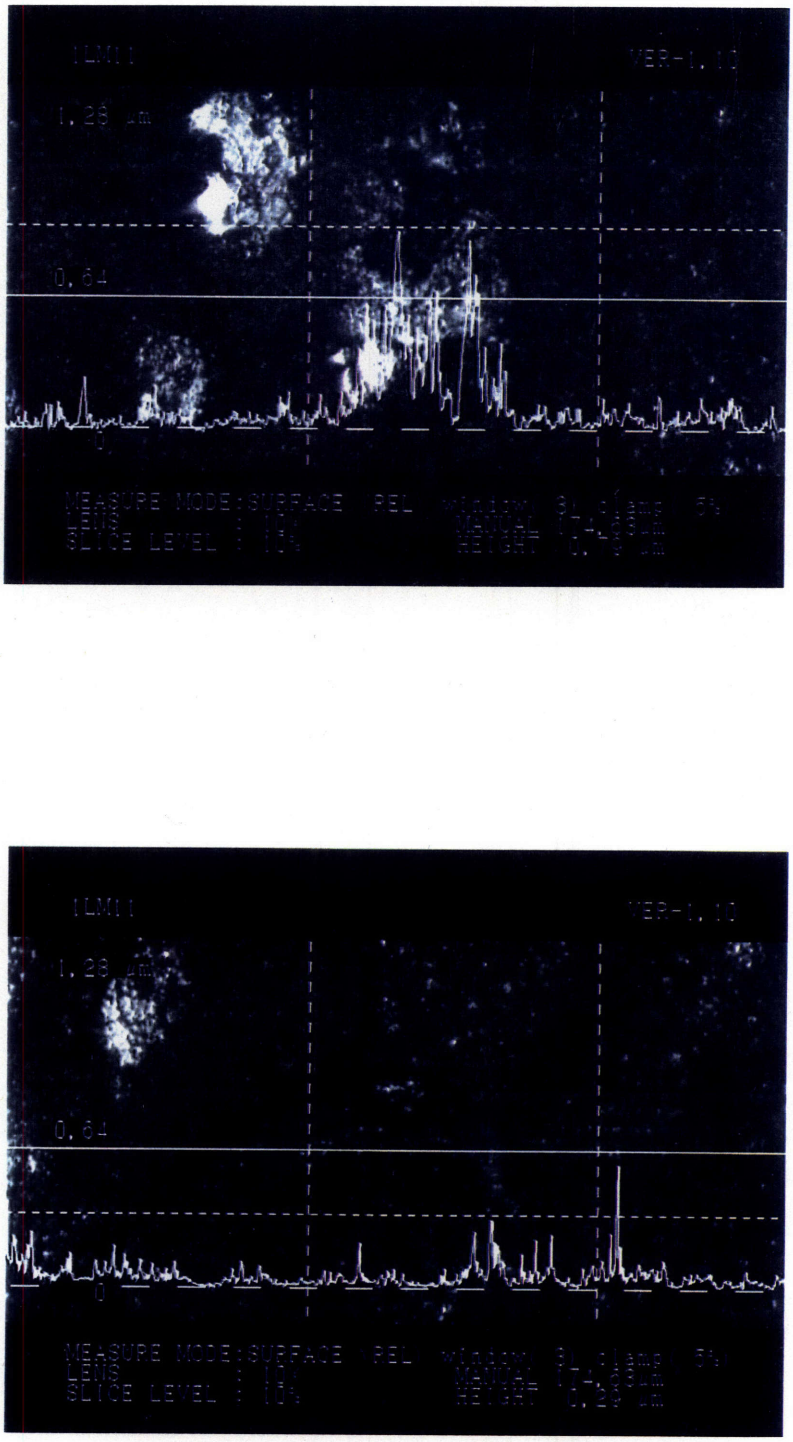

Figure 4.38: Laser Microscope measurement of corresponding point on other half of fractured sample

Chapter 5

Discussion

5.1 Video Microscope

The video microscope is a useful tool for the study of fractures of these types of joints. The ability to make a continuous record makes it possible to observe the entire test. Therefore, any point of interest on the load graph can then be compared with the video record. Alternatively, a review of the tape that raises questions can be compared with the load graph. For example, if cracking is observed at a certain time, that point on the load graph can then be examined for the beginnings of non-linear behavior.

All three types of failure that are commonly exhibited by adhesive lap joints in fiber reinforced composite materials were seen in this series of tests. The results can be summarized in the following table.

Failure Type	Hysol	Plexus	Gougeon
Interlaminar	X		
Cohesive		X	
Adhesive			X

Table 5.1: Failure Type of Sample

The results of this examination have revealed some interesting points about the behavior of adhesive lap joints. Finite element analysis has predicted a high stress concentration at the tips of a lap joint, and the stress is in a Mode I direction[13]. This was confirmed by the results of the tests, particularly the Hysol samples. The cracking behavior of the Hysol samples indicates Mode I failure. The cracks initiated outside of the actual overlap. The cracks opened in a direction normal to the crack elongation direction. The initiation of the crack outside of the joint is particularly interesting. This suggests that

the opening of the crack is due to the much less stiffness of the adherend as compared to the stiffness of the joint area itself, as stiffness of a member is related to the second moment of inertia:

$$I = \frac{bh^3}{12}. \tag{5.1}$$

Equation 5.1 is the equation for a rectangular cross-section[22]. Consequently, the stiffness of the joint area is approximately eight times the stiffness of the adherend. The joint would tend to stay undistorted, while the moment created by the couple of the adherend centroid mismatch (see fig. 3.1) would tend to distort the much less stiffer adherend adjacent to the joint. As a consequence, interlaminar failure occurred between the 0^o and the 90^o plies. Due to the brittle nature of the epoxy adhesive, the two adherends would tend to act as one, thicker piece.

The Plexus samples exhibited a more complicated behavior, but they too eventually failed in at least a partial peel mode. The samples all exhibited some initial sliding, but eventually a Mode I failure would begin. The failures all occurred within the adhesive, it was cohesive failure. The flexible nature of the Plexus adhesive appeared to not transmit as much of the bending moment, the approximation of the two adherends as one rigid piece with much higher stiffness than the adherend is not really valid here. The stress concentration at the ends of the joint was confirmed by the greater distortion of existing flaws such as voids. If these voids were large enough, they could act as an origin for a crack, as was observed in figure 4.28. When a crack actually occurred, it was observed to initiate at or near the end of the joint, and always within the adhesive. The crack would then open, and propagate into the joint, as would be expected from the moment generated by the couple, which is still present.

The Gougeon samples were not well suited to the use of the video microscope. This is due to the type of failure. The adhesive failure exhibited no visible cracking or distortion, and then suddenly failed. This sudden failure the video microscope is not capable of recording, or at least not on a standard VCR.

The results of this study have ramifications for the design of composite joints, reinforcing some empirically determined design rules. The stress concentration at the ends of the joint was clearly exhibited. In both the Hysol and Plexus samples, the fracture always initiated at the ends, and it is likely that the failure of the Gougeon samples also occurred at the ends. Reducing this stress concentration is important. A common technique used is to taper the laminate towards the end of the joint. This would have the effect of gradually changing the stiffness in the area of the joint, rather than abruptly changing the stiffness. The behavior of sample **h2**, which had the longest spew fillet, supports the theory that it is the lower stiffness of the individual adherend which causes the crack to initiate outside of the joint. In the **h2** sample, the crack initiated outside the joint, under the spew fillet, as if the spew fillet itself increased the stiffness slightly. A finite element analysis of the adhesive adherend interface in fiber reinforced composites conducted by Pradhan and colleagues concluded that a high thickness ratio was desirable[14]. This thickness ratio was the ratio of adherend thickness to adhesive thickness. This would have the effect of reducing the couple due to the mismatch of adherend centroids. Reducing the couple would reduce the bending moment in the vicinity of the joint. Reducing the bending moment would reduce the peeling stresses, which the video microscope showed are present and responsible for the cracking of the adherends. Pradhan's work was with a double lap joint, but the basic peel problem at the end of the joint would still be present.

The results of this study indicate that end details do matter for the initiation of a crack. All of the failures observed originated at the end of the joint, whether the failure occurred in the laminate or the adhesive. With the Hysol samples, the cracks were observed to initiate just outside of the joint. The drastic change in stiffness resulting in a stress concentration at the end would account for this. The greater opening of the crack outside of the immediate joint area is an indicator of the effects of this stiffness change.

The laser microscope results were unfortunate. It is believed that the problem with measuring a mismatch was the very severe roughness of the surface of the Plexus samples after cohesive failure. In addition, there seemed to be considerable elastic recovery in the Mode II direction of the Plexus adhesive after Mode I failure occurred. This recovery could be seen by the straightening of the reference marks wherever a Mode I crack had occurred.

5.2 Comments on the Experimental Technique

The experiments in general went well. The video microscope was well suited to the task of forming a continuous record of the test. As with any experiment, there are several suggestions that can be made for future users of this equipment:

1) The video microscope has no automatic scale feature. To make measurements of distortion or cracks simpler, include a record of a scale rule at the beginning of the record. This is important as the magnification on the lens is calibrated to a 12 inch diagonal monitor, so any prints made from the tape will not have a magnification corresponding to the value indicated on the lens.

2) Strain measurements of these types of joints would be difficult to do with typical strain gauges. Strain data was not recorded for this series of experiments. A printed grid

on the edge of the joint, along with an included scale rule, would allow the measurement of displacements, and, consequently, the strain.

3) When taking images of CFRP samples, contrast can be a problem. It could be worthwhile to lighten the edges of the samples with paint or light dye.

4) High magnifications are not required to achieve good results. A lower magnification allows more of the sample to be observed. A magnification of 40X on the monitor was found to be adequate, it allowed the entire width of the joint to be observed, and a good portion of the length was in view.

Chapter 6

Conclusion

An investigation was performed into the application of a video microscope for the study of adhesive lap joints in FRP's. The actual samples used were CFRP, with three separate adhesives. It was found that the video microscope is a good tool for the study of these types of joints if the failure exhibits any yielding behavior. If the material failed in a brittle fashion, the failure was too fast to record. Three types of failure were observed, adhesive, cohesive, and interlaminar. Adhesive failure occurred in a brittle fashion, but both the cohesive and interlaminar failures were capable of being observed with the video microscope.

A literature search was made to assess the state of the art in adhesive joint research. While there has been considerable study of adhesive joints, both with composite adherends and isotropic adherends such as metals, there have not been any real time studies of the failure of composite. The video microscope provided this capability.

The results of this study provided confirmation of conclusions drawn from other techniques. FEM techniques predict a great stress concentration at the ends of lap joints. These stress concentrations could be seen in the initiation of failure always being at or near the ends of the joints. Due to the eccentricity of the load path, in that adhesives have to transfer stresses in shear, necessitating an overlap of some type, there will be a bending moment on the joint resulting in peel stresses at the end of the joint. These peel stresses were clearly exhibited in these experiments. Even the very ductile Plexus samples, while distorting in the Mode II direction initially, eventually exhibited crack formation and opening indicative of peel stresses.

References

[1] Mukhopadhyay, S. K. "High Performance Fibres; Chap.3.5 - Carbon Fibre Properties; Chap.3.6 - Carbon Fibre Applications and New Developments." *Textile Progress*, 25(3/4), pp.29-36

[2] John, S.J., Kinloch, A.J., Matthews, F.L. "Measuring and Predicting the Durability of Bonded Carbon Fibre/Epoxy Composite Joints." *Composites*, **22**(2), March, 1991, pp.121-127

[3] Overd, Michael L. "Carbon Composite Repairs of Helicopter Metallic Primary Structures." *Composite Structures,* **25**, 1993, pp. 557-565

[4] Heslehurst, R.B., Baird, J.P., Williamson, H.M. "The Effect on Adhesion Stiffness due to Bonded Surface Contamination." *Journal of Advanced Materials,* April, 1995, pp.11-15

[5] Dewen, P.N., Cawley, P. "Cohesive Property Determination in Bonded Joints with Composite Adherends." *Measurement*, **11**(4), July, 1993, pp.361-379

[6] Chamis,C.C., Murthy, P.L.N. "Simplified Procedures for Designing Adhesively Bonded Composite Joints." *J. Reinforced Plastics and Composites,* **10**, January, 1991, pp. 29-41

[7] Fernlund, G., Papini, M., McCammond, D., Spelt, J. K. "Fracture Load Predictions for Adhesive Joints". *Composites Science and Technology,* **10**(4), 1994, pp.587-600

[8] Vinson, J.R., "Adhesive Bonding of Polymer Composites." *Polymer Engineering and Science,* **29**(19), Mid-October 1989, pp. 1325-1331

[9] Roberts, T.M., "Shear and Normal Stresses in Adhesive Joints." *Journal of Engineering Mechanics,* **115**(11), November, 1989, pp. 2460-2479

[10] Papini, M., Fernlund, G., Spelt, J.K. "Effect of Crack-Growth Mechanism on the Prediction of Fracture Load of Adhesive Joints." *Composites Science and Technology,* **52**, 1994, pp. 561-570

[11] Chai, Herzl "Shear Fracture." *International Journal of Fracture,* **37**(2), June, 1988, pp. 137-158

[12] Reddy, J.N., Roy, S. "Non-Linear Analysis of Adhesively Bonded Joints." *International Journal of Non-Linear Mechanics,* **23**(2), 1988, pp. 97-112

[13] Mitra, A.K., Ghosh, B. "Interfacial Stresses and Deformations of an Adhesive Bonded Double Strap Butt Joint Under Tension." *Computers and Structures,* **55**(4), 1995, pp.687-694

[14] Pradhan, S.C., Iyengar, N.G.R., Kishore, N.N. "Parametric Study of Interfacial Debonding in Adhesively Bonded Composite Joints." *Composite Structures,* **29**(1), 1994, pp.119-125

[15] Theotokoglou, E.E., Moan, T. "Stress Analysis of a GRP/PVC Sandwich T-Joint." *Composites Design, Manufacturing, and Application, Proceedings of the 8th Int. Conference on Composite Materials*, July, 1991, pp.9-C-1, 9-C-10

[16] Shenoi, R.A., Violette, F.L.M. "A study of Structural Composite Tee Joints in Small Boats." *Journal of Composite Materials,* **24**, june, 1990, pp. 644-666

[17] Shenoi, R.A., Hawkins, G.L. "Influence of Material and Geometry Variations on the Behaviour of Bonded Tee Connections in FRP Ships." *Composites,* **23**(5), Sept., 1992, pp.335-345

[18] Shenoi, R.A., Hawkins, G.L. "An Investigation into the Performance Characteristics of Top-Hat Stiffener to Shell Plating Joints." *Composite Structures,* **30**, 1995, pp. 109-121

[19] American Bureau of Shipping. *Guide for Building and Classing Offshore Yachts* (1986)

[20] Capricorno, 50 foot CFRP sloop, built and rebuilt at Eric Goetz Custom Sailboats, author worked on the construction and repair of the vessel

[21] Gougeon Brothers; *The Gougeon Brothers on Boat Construction*, Fourth Edition, 1985

[22] Popov, Egor P..; *Engineering Mechanics of Solids*